

AperTO - Archivio Istituzionale Open Access dell'Università di Torino

Histamine type 1-receptor activation by low dose of histamine undermines human glomerular slit diaphragm integrity

This is the author's manuscript

Original Citation:

Availability:

This version is available <http://hdl.handle.net/2318/1611478> since 2017-06-20T12:31:02Z

Published version:

DOI:10.1016/j.phrs.2016.10.011

Terms of use:

Open Access

Anyone can freely access the full text of works made available as "Open Access". Works made available under a Creative Commons license can be used according to the terms and conditions of said license. Use of all other works requires consent of the right holder (author or publisher) if not exempted from copyright protection by the applicable law.

(Article begins on next page)

This Accepted Author Manuscript (AAM) is copyrighted and published by Elsevier. It is posted here by agreement between Elsevier and the University of Turin. Changes resulting from the publishing process - such as editing, corrections, structural formatting, and other quality control mechanisms - may not be reflected in this version of the text. The definitive version of the text was subsequently published in PHARMACOLOGICAL RESEARCH, 114, 2016, 10.1016/j.phrs.2016.10.011.

You may download, copy and otherwise use the AAM for non-commercial purposes provided that your license is limited by the following restrictions:

- (1) You may use this AAM for non-commercial purposes only under the terms of the CC-BY-NC-ND license.
- (2) The integrity of the work and identification of the author, copyright owner, and publisher must be preserved in any copy.
- (3) You must attribute this AAM in the following format: Creative Commons BY-NC-ND license (<http://creativecommons.org/licenses/by-nc-nd/4.0/deed.en>), 10.1016/j.phrs.2016.10.011

The publisher's version is available at:

<http://linkinghub.elsevier.com/retrieve/pii/S1043661816310556>

When citing, please refer to the published version.

Link to this full text:

<http://hdl.handle.net/2318/1611478>

1 **Histamine Type 1-Receptor activation by low dose of histamine undermines human**
2 **Glomerular Slit Diaphragm Integrity**

3 *Eleonora Veglia^{a#}, Alessandro Pini^{b#*}, Aldo Moggio^{al}, Cristina Grange^c, Federica Premoselli^d,*
4 *Gianluca Miglio^a, Katerina Tiligada^e Roberto Fantozzi^a, Paul L. Chazot^f, Arianna Carolina Rosa^{a,f}*

5
6 *#Authors contributed equally to this work*

7 *^aDepartment of Scienza e Tecnologia del Farmaco, University of Turin, Via P. Giuria 9 - 10125,*
8 *Turin, Italy, eviglia@unito.it, aldomoggio@gmail.com, rfantozzi@unito.it, acrosa@unito.it;*

9 *^bDepartment of Clinical and Experimental Medicine, University of Florence, Viale Pieraccini 6 -*
10 *50139, Florence, Italy, apini@unito.it; ^cDepartment of Scienze Mediche, University of Turin, C.So*

11 *Dogliotti 14 - 10126 Turin, Italy, cgrange@unito.it; ^dDepartment of Neuroscience "Rita Levi*
12 *Montalcini", University of Turin, Via Cherasco 15, 10126 Turin, Italy, fpremoselli@unito.it;*

13 *^eDepartment of Pharmacology, Medical School, University of Athens, M. Asias 75 GR-115 27*
14 *Athens, Greece, aityliga@med.uoa.gr; ^fSchool of Biological and Biomedical Science, Durham*

15 *University, Durham DH13LE, UK, paul.chazot@durham.ac.uk*

16

17 ***Corresponding author:** Alessandro Pini, PhD

18 Dipartimento di Medicina Sperimentale e Clinica Sezione di Anatomia e
19 Istologia Università degli Studi di Firenze,

20 Viale Pieraccini 6, 50139, Florence, Italy

21 Phone: +390552758155

22 e-mail: alessandro.pini@unifi.it

23 ¹ Present affiliation: Integrated Cardio Metabolic Centre, Department of Medicine, Huddinge
24 (MedH), H7, Karolinska Institute, SE-171 77 Stockholm, Sweden

25 **Abstract**

26 Histamine has been reported to decrease the ultrafiltration coefficient, which inversely correlates
27 with glomerular permselectivity, however the mechanism(s) underling this effect have never been
28 investigated. This study aimed to assess whether histamine could exert a direct detrimental effect on
29 podocyte permeability and the possible involvement of two key proteins for the glomerular slit
30 diaphragm (SD) integrity, zonula occludens-1 (ZO-1) and P-cadherin.

31 The effect of histamine (100 pM-1000 nM) on coloured podocytes junctional integrity was
32 evaluated functionally by a transwell assay of monolayer permeability and morphologically by
33 electron microscopy. Histamine receptor (H₁₋₄R) presence was evaluated at both mRNA (RT-PCR)
34 and protein (immunofluorescence) levels. The K_d and B_{max} values for [³H]mepyramine were
35 detemined by saturation binding analysis; IP₁ and cAMP production evoked by histamine were
36 measured by TR-FRET. ZO-1, P-cadherin and vimentin expression was assessed by qRT-PCR and
37 quantitative immunoblotting.

38 Histamine elicited a time- and sigmoidal dose-dependent (maximum effect at 8 h, 10 nM) increase
39 in podocyte paracellular permeability widening the paracellular spaces. Only H₁R was
40 predominantly localised to the podocyte membrane. Consistently, histamine elicited a sigmoidal
41 dose-dependent increase in IP₁, but not in cAMP. Histamine exposure evoked a concentration-
42 dependent reduction in both ZO-1 and P-cadherin and a parallel induction of vimentin mRNA
43 expression with a maximum effect after 6 h, and protein expression with a maximum effect after 8h.
44 These effects were prevented by the selective H₁R antagonist chlorpheniramine.

45 In conclusion, our data demonstrate that histamine, via the H₁R, modifies SD morphological and
46 functional integrity, in part, by decreasing the expression of ZO-1 and P-cadherin.

47

48 **Keywords:** histamine, podocytes, paracellular permeability, histamine receptors, junction integrity.

49 **Abbreviations** cAMP, cyclic adenosine monophosphate; *CDH3*, cadherin 3, type 1, P-cadherin
50 gene; ER, endoplasmic reticulum; FITC, fluorescein; *GADPH*, glyceraldehyde 3-phosphate
51 dehydrogenase gene; GBM, glomerular basement membrane; H₁₋₄R, histamine receptor 1-4 subtypes;
52 K_f, ultrafiltration coefficient; IP₁, inositol monophosphate; IP₃, inositol 1,4,5-trisphosphate; PAN,
53 puromycin aminonucleoside; qRT-PCR, quantitative real-time PCR; SD, slit diaphragm; TBP,
54 TATA-binding protein; *TJPI*, tight junction protein 1 gene; TR-FRET, Time-Resolved
55 Fluorescence Resonance Energy Transfer; *VIM* vimentin gene; ZO, Zonula Occludens

56

57 **1 Introduction**

58 Histamine is a pleiotropic vasoactive amine, whose pathogenic role in microvascular endothelial
59 paracellular permeability has been extensively studied [1-7]. Most of these studies describe acute
60 events (within seconds to minutes), resulting in a rapid transient increase in permeability, due to a
61 rapid formation of endothelial gaps [2-7]. Moreover, histamine has been suggested to be involved in
62 prolonged vascular leakage by reducing Zonula Occludens (ZO)-1 protein expression in cultured
63 retinal microvascular endothelial cells within hours [8]. The work by Takeuchi K and colleagues
64 (2001) suggested that histamine-induced paracellular permeability might be also extended to other
65 epithelial cells. In particular, histamine was shown to significantly downregulate ZO-1 mRNA
66 expression in cultured human nasal epithelial cells [9]. ZO-1 contributes to the functional integrity
67 of different permeability barriers among which the glomerular filter is one [10]. Interestingly,
68 histamine has been previously reported to decrease the ultrafiltration coefficient (K_f) [11]. Thus, our
69 hypothesis was that histamine could modify K_f by regulating ZO-1 expression in the podocyte.

70 Podocytes are parenchymal cells known to be highly dynamic and terminally differentiated. They
71 interact with the glomerular basement membrane (GBM) and communicate through various
72 signalling pathways at the slit diaphragm (SD). The glomerular SD represents the junction structure
73 that links the interdigitating foot processes from neighbouring podocytes and consists of
74 transmembrane-bridging proteins networking with a juxtaposed cytoplasmic platform of protein

75 complexes, which in turn is linked to the actin cytoskeleton [12]. Within this cytoarchitecture, ZO-1
76 protein is located at the cytoplasmic face of the SD [13] and has been accepted to be one of its
77 functional molecules; a disrupted interaction and distribution of ZO-1 in podocytes results in loss of
78 SD structure and function [14-16]. Besides the transmembrane protein, P-cadherin, a podocyte
79 specific adhesion protein [17] localised on adherens-type junctions, mediates calcium-dependent
80 cell-cell bonds and its loss is recognised as a cause of barrier filtration integrity impairment [18].
81 Therefore, it is likely that glomerular injury affecting ZO-1 and/or P-cadherin results in loss of SD
82 structure, podocyte detachment, K_f reduction and in a subsequent impairment of the filtration
83 barrier integrity with proteinuria, progressive renal damage and eventual loss of renal function [12,
84 19, 20].

85 Among the histamine receptor subtypes, $H_{1-4}R$, H_1R and H_2R were first described in mammalian
86 glomeruli [21-23], but these studies were focused on the entire glomerulus or only on stromal cells
87 such as mesangial cells; little is known about parenchymal cells. Indeed, the data on histamine
88 receptors expression on renal parenchymal cells arise only from our recent observations of H_1R ,
89 H_2R , H_3R and H_4R on tubular epithelial cells [24-26]. However, no such studies have to date
90 focused on podocytes.

91 Thus, the present study was designed to investigate whether histamine could exert a direct
92 detrimental effect on podocyte permeability compromising SD functional integrity, the underlying
93 histamine receptor pharmacology, and the possible involvement of two key SD-associated proteins
94 ZO-1 and P-cadherin.

95 **2 Materials and Methods**

96 ***2.1 Materials***

97 All reagents and chemicals used were from Sigma–Aldrich (St. Louis, MO) unless otherwise noted.
98 Cell media and reagents were from Lonza group Ltd. (Allendale, NJ, USA). Hans Balanced Salt
99 Solution was from GIBCO (Grand Island, NY). HTS Transwell inserts were from Corning Life

100 Sciences (Lowell, MA). RevertAid™ First Strand cDNA Synthesis Kit, GeneRuler™ 50 bp DNA
101 Ladder, DNA Gel Loading Dye (6X), CellMask™ Orange plasma membrane stain, MagicMark™
102 XP Western Protein Standard and Alexa-Conjugated secondary antibodies donkey anti-Mouse IgG
103 (A-31570), chicken anti-Goat IgG (A-21469) and goat anti-Rabbit IgG (A-11034) were from
104 Thermo Fisher Scientific Inc. (Rockford, IL, USA). EuroTaq DNA polymerase as well as
105 EuroGOLD Trifast™ were from Euro-clone (Milan, Italy). High Capacity cDNA Reverse
106 Transcription Kit and Power SYBR Green PCR Master Mix were from Applied Biosystems (Foster
107 City, CA). Sequence-specific oligonucleotide primers were purchase from Sigma-Genosys (Milan
108 Italy). The antibodies for histamine H₁R (H300, sc-20633), H₂R (A20, sc-33973), calnexin (AF18,
109 sc-23954), ZO-1 (C-19, sc-8146), P-cadherin (H-105, sc-7893), vimentin (C20, sc-7557) and
110 UltraCruz™ Autoradiography Film were purchased from Santa Cruz Biotechnology Inc. (Dallas,
111 TX, USA), while anti-rabbit and anti-mouse IgG HRP-linked antibodies were from Cell Signaling
112 Technology, Inc. (Danvers, MA, USA) and the swine anti-Goat IgG antibody from Cedarlane Labs
113 (Ontario, Canada). The LANCE® Ultra cAMP Detection Kit, the IP-One HTRF® assay kit, the
114 [³H]mepyramine [PubChemCID 656400; kindly provided by Prof. Rob Leurs (20 Ci/mmol) VU
115 University Amsterdam, Amsterdam] and the Whatman™GF/C Glass Fiber Filter Paper were from
116 PerkinElmer Inc. (Waltham, MA, USA) and Cisbio Bioassays (France), respectively. Precision Plus
117 Protein™ Dual Color Standards and BCA protein assay were from Pierce Bio-technology Inc.
118 (Rockford, IL, USA) and PVDF membrane from Millipore (Bradford, MA, USA). Visiglo™ HRP
119 chemiluminescent substrate kit was purchased from Amresco llc. (Solon, OH, USA).

120 Histamine dihydrochloride (PubChem CID 5818), (+/-) chlorpheniramine maleate (PubChem CID
121 5281068), [³H]mepyramine and difenhydramine (Pubmed CID 3100) were dissolved in dimethyl
122 sulfoxide, and the final drug concentrations were obtained by dilution of stock solutions in the
123 experimental buffers. The final concentration of the organic solvent was less than 0.1%, which had
124 no effect on cell viability.

125 **2.2 Cell cultures**

126 Immortalised human podocytes were obtained from the respective primary cells, derived from the
127 normal portion of cortex surgically removed kidneys (n=5) for as described previously [27], by
128 infection with a hybrid Adeno5/SV40 virus as previously described [27-29]. **The line was generated**
129 **in 1997, after the authorization of the local Ethical Committee (Hospital San Giovanni Battista**
130 **"Molinette", Turin, Italy). Podocytes were isolated from the healthy tissue derived from kidney**
131 **samples of patients who underwent unilateral nephrectomy due to local renal carcinomas as first-**
132 **line treatment. To our knowledge, no other relevant pathology was diagnosed in the medical history**
133 **of each patient enrolled and the derived podocytes can be reasonable assumed as healthy podocytes.**
134 Podocytes were characterised for the positive expression of nephrin, podocin, and synaptopodin and
135 for negative expression of von Willebrand factor, CD31, and smooth muscle cell actin. Cells were
136 cultured in DMEM containing 4.5 mg/l glucose supplemented with 10% Fetal Calf Serum,
137 penicillin/streptomycin (100 IU/ml), and l-glutamine and the cultures were maintained at 37 °C in a
138 95% air/5% CO₂ humidified incubator.

139 ***2.3 Permeability assay***

140 Podocyte monolayer permeability was determined as previously described [30, 31]. Human
141 immortalised podocytes (40,000 cells well, 500 µl) were seeded on the top of HTS Transwell inserts
142 (3 µm pore, 24-well plate) and cultured till confluence was achieved. Cells were washed twice with
143 PBS supplemented with 1 mM MgCl₂ and 1 mM CaCl₂ and then pre-treated with vehicle alone or
144 chlorpheniramine maleate 10 µM for 10 min before exposure to histamine 0.01-1000 nM for 0-8 h.
145 Fluorescein (FITC)-labeled bovine serum albumin was added to the bottom chambers of the
146 transwells and medium fluorescence activity in the top chambers was measured at selected time-
147 points with a fluorescence plate reader (excitation: 495 nm, emission: 520 nm; multiple plate reader
148 Victor X4; PerkinElmer Inc.). Fold-change in expression with respect to the control mean was
149 calculated for all samples.

150 ***2.4 Electron microscopy***

151 Podocytes pre-treated with vehicle alone or chlorpheniramine maleate 10 μ M for 10 min before
152 exposure to histamine 10 nM or 0.1 nM for 0-8 h were fixed in 4% glutaraldehyde and post-fixed,
153 after pelleting, in 1% osmium tetroxide and embedded in Epon 812. Ultrathin sections were stained
154 with uranyl acetate and alkaline bismuth subnitrate and examined under a JEM 1010 electron
155 microscope (Jeol, Tokyo, Japan) at 20 kV and 50 kV. Morphometrical analysis were performed on
156 50KV digitized images using ImageJ 1.41 software (<http://rsbweb.nih.gov/ij>; NIH, USA) in 20
157 regions of interest (ROI) for each sample.

158 **2.5 RT-PCR**

159 Two μ g/ μ l of total RNA extracted from podocytes by using RevertAid™ First Strand cDNA
160 Synthesis Kit according to the manufacturer's instruction, were subjected to RT-PCR as previously
161 described [26, 32]. The subsequent specific oligonucleotide sequences were used: *hH1R* forward 5'
162 CATTCTGGGGGCCTGGTTTCTCT-3' and reverse 5'-CTTGGGGGTTTGGGATGGTGACT-3';
163 *hH2R* forward 5'-CCCGGCTCCGCAACCTGA-3' and reverse 5'-
164 CTGATCCCGGGCGACCTTGA-3'; *hH3R* forward 5'-CTTCCTGCCCTAGCAGTT-3' and reverse
165 5'-GCAGAGAACAGCTTCGAGGTT-3' *hH4R* forward 5'-TGGAAGCGTGATCATCTCAG-3'
166 and reverse 5'-ATATGGAGCCCAGCAAACAG-3'. PCR amplicons were resolved in an ethidium
167 bromide-stained agarose gel (2.5%) by electrophoresis. GAPDH gene expression was used as an
168 internal control.

169 **2.6 Immunocytofluorescence and confocal analysis**

170 Podocytes plated on collagen-coated cover glasses were fixed with 4% paraformaldehyde for 10
171 minutes at room temperature. H₄R was detected using The anti-hH₄R (374–390) antibody produced
172 and validated for detecting both human and rodent H₄R in the School of Biological and Biomedical
173 Sciences, Durham University [33-39]. Sections were incubated overnight with anti-H₁R (1.3
174 μ g/ml), anti-H₂R (1.3 μ g/ml) or anti-H₄R (2 μ g/ml) receptor subunit at 4°C. Subsequently, for
175 endoplasmic reticulum (ER) cells were incubated with anti-calnexin (2 μ g/ml) followed by

176 incubation with the respective Alexa-Conjugated secondary antibodies. **The negative control to**
177 **exclude non-specific staining by the secondary antibody (where cells were incubated with**
178 **secondary antibodies alone) is reported in Supplementary Material Fig. 1.** The plasma membrane
179 was stained using CellMask™ Orange plasma membrane stain according to the manufacturer's
180 protocol. Cells were fixed with 4% paraformaldehyde and processed for histamine receptors
181 staining. Nuclei were stained with Hoescht. All the slides were examined at ×63 magnification using
182 the SP5 Confocal Laser Scanning Microscope SMD (Leica). A variable number of optical section
183 images in the z-dimension (z-spacing, 0.42μm) were collected ensuring that images throughout the
184 3D cellular structure, spanning multiple confocal planes, were fully captured. Maximum projection
185 of the confocal images were analyzed quantitatively for the extent of colocalization of H₁₋₄Rs with
186 each of the sub-compartment marker proteins using the ImageJ software package.

187 ***2.7 Radioligand binding studies***

188 The saturation binding isotherms were determined by incubating washed podocyte homogenates for
189 45 min at 25°C with 0–16 nM [³H] mepyramine and assay buffer (50 mM phosphate buffer pH 7.4)
190 in a total assay volume of 200 μl. The incubation was stopped by rapid dilution with ice-cold assay
191 buffer. Non-specific binding was determined using unlabelled 10 μM difenhydramine. The bound
192 radioactivity was separated by filtration through GF/B Glass Fiber Filter Paper that had been treated
193 with 0.3% polyethyleneimine (PEI). Filters were washed thrice with ice-cold assay buffer and the
194 radioactivity retained on the filters was measured by liquid scintillation counting. Protein
195 concentrations were determined according to Bradford methods, using bovine serum albumin as a
196 standard.

197 ***2.8 Time-Resolved Fluorescence Resonance Energy Transfer (TR-FRET)***

198 The TR-FRET assay was used to evaluate both cAMP and IP₁ production by using the LANCE®
199 Ultra cAMP Detection Kit and the IP-One HTRF® assay kit, respectively, as previously described
200 [26] and according to their manufacturer's instruction. The energy transfer was measured by the
201 multiple plate reader Victor X4 (excitation: 620 nm, emission: 665 nm).

202 **2.9 Quantitative real-time PCR (qRT-PCR)**

203 qRT-PCR was performed on RNA isolated by EuroGOLD Trifast™ according to the
204 manufacturers' instructions from podocytes (80% confluence) pretreated with vehicle alone or with
205 chlorpheniramine maleate at 10 μM and challenged with histamine in the range 3 pM-1000 nM for
206 0-8 and 24 h. Briefly, first-strand cDNA was produced from 200 ng of total RNA using the High
207 Capacity cDNA Reverse Transcription Kit. Real-time PCR experiments were performed in 20-μl
208 reaction mixture containing 5 ng of cDNA template, the sequence-specific oligonucleotide primers
209 (*TJP1* forward: CATCAGATCATTCTGGTCGATCA and reverse: TCCGGAGACTGCCATTGC;
210 *CDH3* forward: CCAGCTTGGGCAACATAGGGT and reverse:
211 TCAGCTCCCGCTGAGACTACA; *VIM* forward: GGAACAGCATGTCCAAATCGAT and
212 reverse: CAGCAAACCTTGGATTTGTACCATT), and the Power SYBR Green PCR Master Mix.
213 TATA-binding protein (TBP) mRNA were used to normalise RNA inputs. The relative expression
214 of mRNA was calculated according to the $2^{(-\Delta Ct)}$ method. Fold-change expression with respect to
215 control was calculated for all samples.

216 **2.10 Immunoblotting**

217 Sixty μg of proteins, extracted by EuroGOLD Trifast™ according to the manufacturers'
218 instructions from podocytes (80% confluence) exposed to vehicle alone or pretreated with vehicle
219 alone or with chlorpheniramine maleate and challenged with histamine in the range 3 pM-1000 nM
220 for 0-8 and 24 h, were subjected to SDS-PAGE using a 8 % gel. The PVDF membrane was blotted
221 over-night with goat polyclonal anti-ZO-1, rabbit polyclonal anti-P-cadherin or goat polyclonal
222 anti-vimentin antibodies (1 μg/ml in PBS) and then re-probed with mouse monoclonal anti-β-actin
223 antibody (1:5000) to confirm the homogeneity of the proteins loaded. The membranes were
224 overlaid with Visiglo™ HRP chemiluminescent substrate kit and then exposed to Hyperfilm ECL
225 film. Densitometric analysis was performed by ImageJ software package. Fold-change expression
226 with respect to control was calculated for all samples.

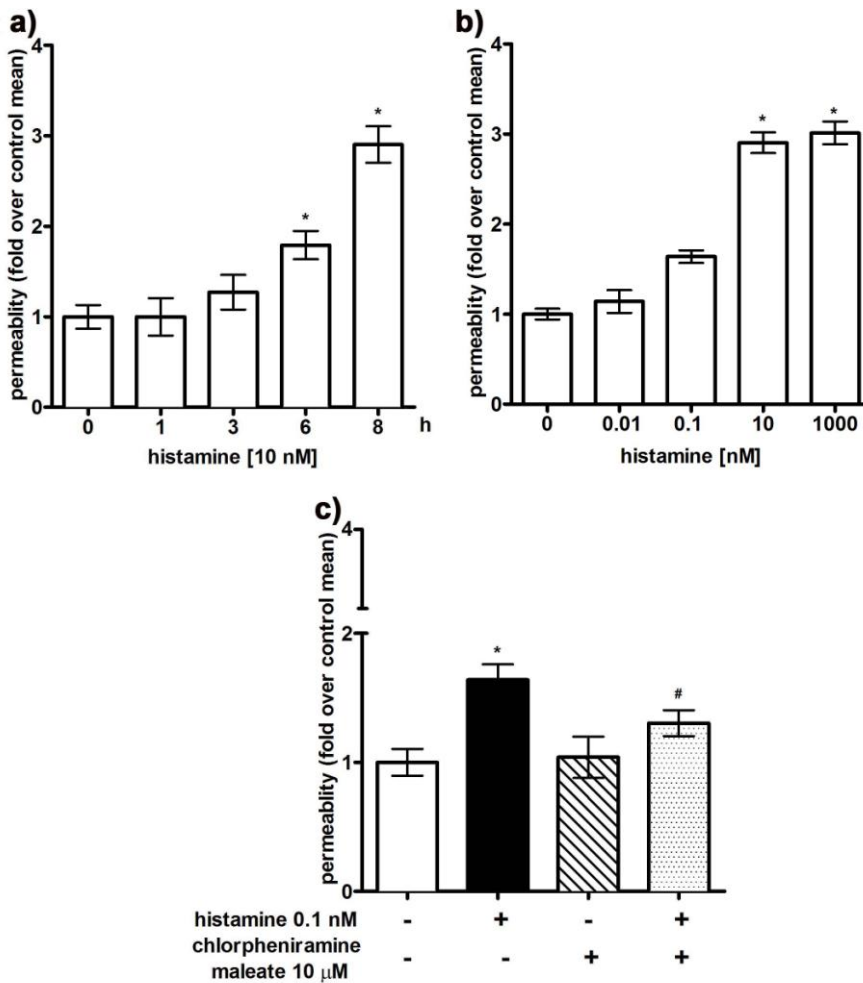
227 **2.11 Data analysis and statistical procedures**

228 Gene and protein expression data are expressed as fold-changes relative to the control (vehicle
229 alone), which is represented as one-fold. For the permeability assay the mean of the control values
230 have been calculated and all the individual control values and all the individual test values are
231 expressed as fold-change relative to the control mean. Results are shown as mean \pm SEM from 5
232 different experiments, and were analysed by Prism 4 software from Graphpad (CA, USA). The test
233 for normality using the Kolmogorov-Smirnov followed by the one-way ANOVA and the *post-hoc*
234 Dunnett's multiple comparison were performed when there was a variance homogeneity
235 (permeability assay). In all the other cases, the non-parametric Kruskal-Wallis test was used. For
236 concentration-response curves a four-parameter logistic equation was applied and the best-fit was
237 obtained. Radioligand binding data were evaluated by a nonlinear, least-squares curve-fitting
238 procedure using GraphPad Prism 5. To determine significant differences between means, the
239 threshold for statistical significance was set to *P*-values < 0.05 .

240 **3 Results**

241 ***3.1 Histamine compromises SD integrity in human immortalised podocytes***

242 We tested whether the amine influences the transepithelial flow of FITC-albumin in a transwell
243 assay of monolayer permeability. We found that histamine treatment (0.01-10 nM; 0-8 h) time- and
244 concentration-dependently and significantly increased fluorescence intensity in the top chamber
245 beginning from 6 h (basal level of Fluorescence intensity = 15651 ± 950 FU; *P* < 0.05) up to 160%
246 at 8 h (*P* < 0.01 ; Fig. 1a) with an EC_{50} of about 0.1 nM (Fig. 1b). Notably, the 10 min pre-treatment
247 of podocytes with chlorpheniramine maleate was effective in preventing the transepithelial flow of
248 FITC-albumin, as demonstrated by its ability to partially prevent the effect exerted by histamine 0.1
249 nM (Fig. 1c).

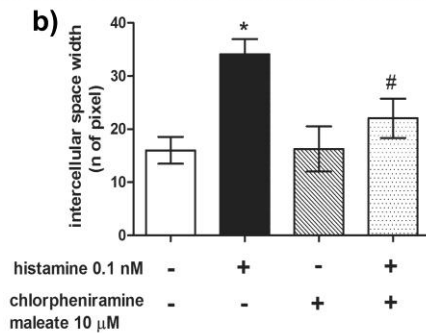
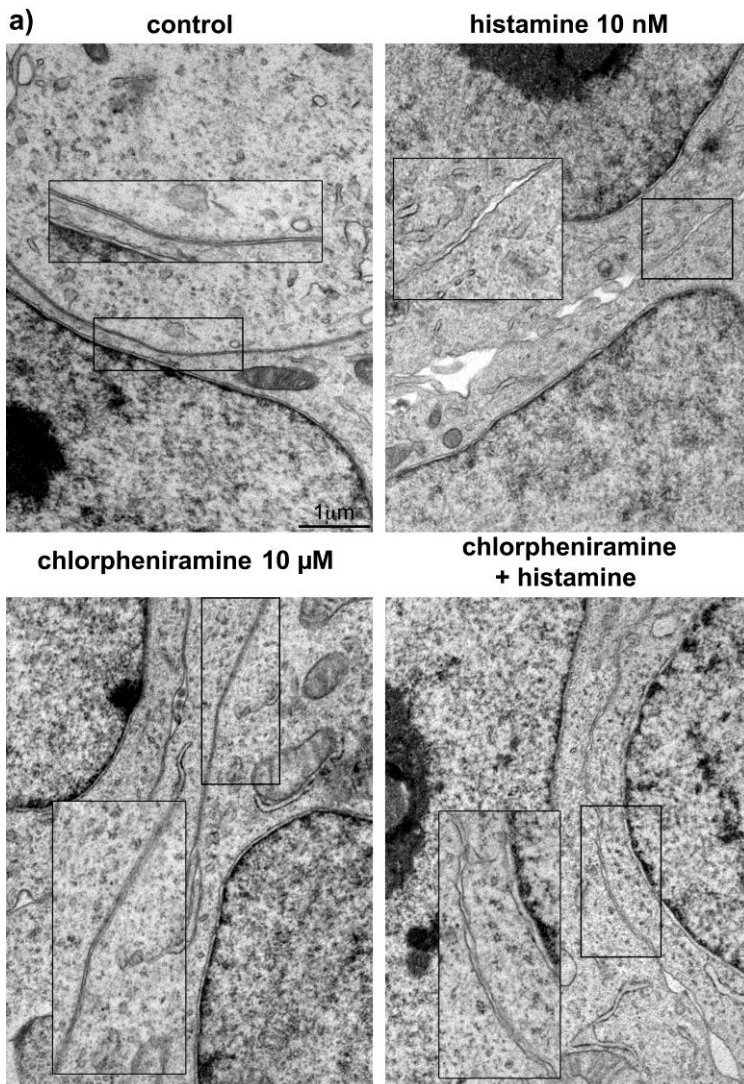


250

251 **Fig. 1. Junction functional integrity of human immortalized podocyte.** Transepithelial albumin
 252 permeability of podocyte monolayer was measured using FITC-BSA. **(a)** Cells were exposed to
 253 histamine 10 nM from 0 to 8 h. Data, expressed as fold-change over control mean, are means ±
 254 SEM of 5 independent experiments. Statistical analysis was performed by one-way ANOVA and
 255 Dunnett test. * $P < 0.05$ versus time 0. **(b)** Cells were exposed to histamine 0 - 1000 nM for 8 h.
 256 Data, expressed as fold-change over control mean, are means ± SEM of four independent
 257 experiments. Statistical analysis was performed by one-way ANOVA and Dunnett test. * $P < 0.05$
 258 versus concentration 0. **(c)** Podocytes pretreated for 10 min with vehicle alone or the selective H₁R
 259 antagonist, chlorpheniramine maleate 10 μM, were exposed to histamine (0.1 nM) for 8 h. Data,
 260 expressed as fold over control, are means ± S.E.M. of 5 independent experiments. * $P < 0.05$ versus
 261 vehicle alone and # $P < 0.05$ versus histamine 0.1 nM.

262

263 The detrimental effect of H₁R activation on SD was strongly validated when the junction integrity
264 was quantitatively evaluated by electron microscopy. The width of the intercellular space was
265 narrow and constant throughout the contact area in the control cells (Fig. 2a and b) whereas it was
266 significantly compromised after histamine exposure for 8 h at 0.1 nM (Fig. 2b), appearing to be
267 discontinuous and uneven with widening of the paracellular spaces after histamine exposure for 8 h
268 at 0.1 nM. The pre-treatment with chlorpheniramine maleate was able to ameliorate the histamine
269 evoked-effects as intercellular spaces appeared narrower, although this was incomplete (Fig. 2a and
270 b). Chlorphenamine treatment alone did not affect the intercellular contact area.



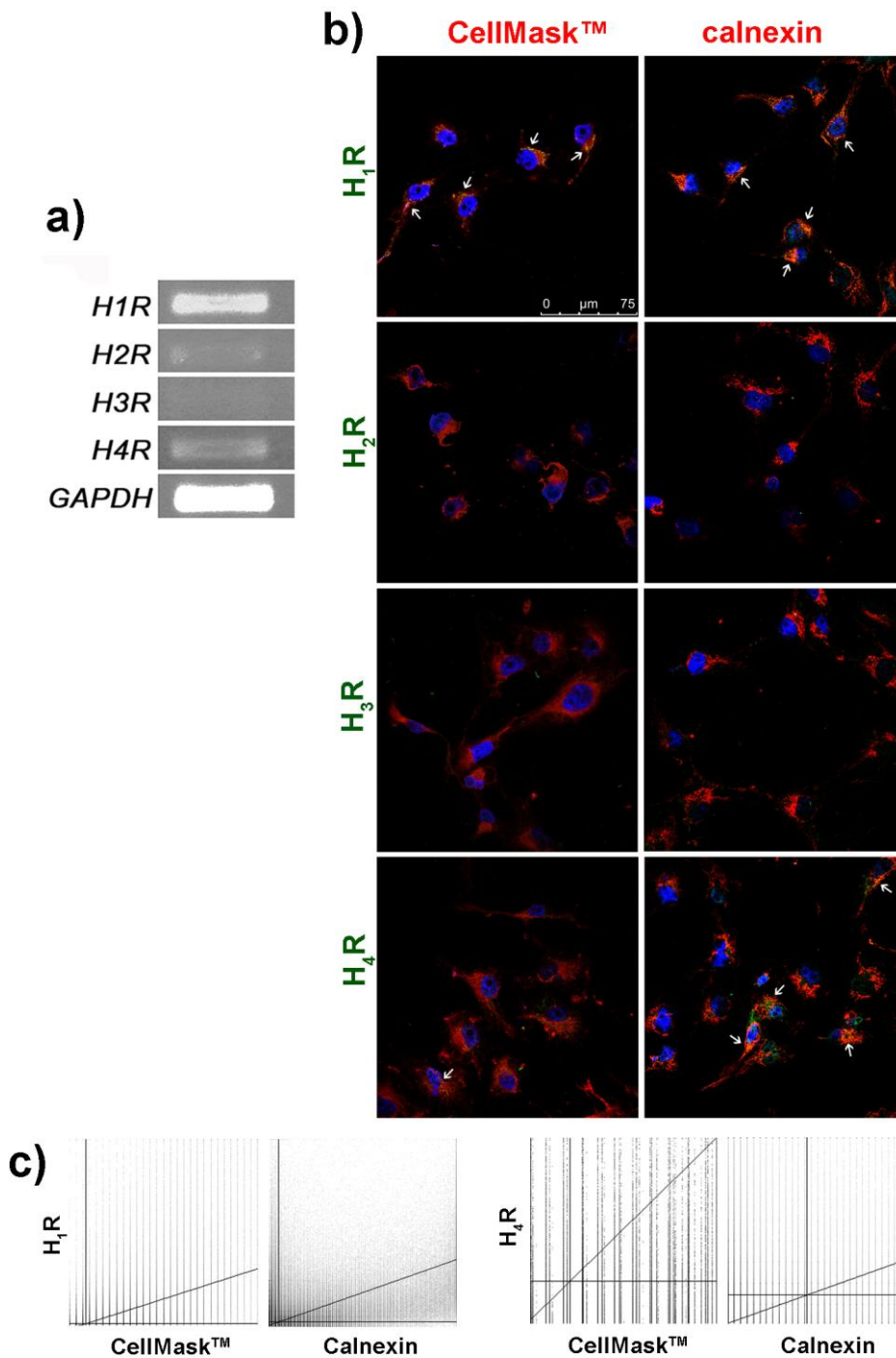
271

272 **Fig. 2 Chlorpheniramine effect on junction integrity.** (a) Representative images of ultrathin
 273 sections from human immortalized podocytes pretreated for 10 min with vehicle alone or the
 274 selective H₁R antagonist, chlorpheniramine maleate 10 μM, were exposed to histamine (0.1 nM) for
 275 8 h. The morphological assessment of the junction integrity was carried out in three different
 276 experiments. Sections were examined under a JEM 1010 electron microscope at 20 kV. The insets
 277 show the integrity junctional level detail evaluated at 50 kV. (b) Quantitative analysis of the

278 intercellular junction morphology performed on 50KV digitized images. Data, expressed as fold-
279 change over control, are means \pm S.E.M. for $n = 20$ regions of interest (ROI) for each sample. $*P <$
280 0.05 versus vehicle alone and $\#P < 0.05$ versus histamine 0.1 nM.

281 282 **3.2 Histamine receptor expression in human immortalised podocytes**

283 In order to further explore the underlying histamine pharmacology, the expression of histamine
284 receptors in human immortalised podocytes was evaluated at both the gene and protein levels.
285 Moreover, their functional expression was confirmed by TR-FRET assay evaluating the second
286 messenger production induced by histamine. As shown in Fig. 3a, RT-PCR analysis revealed single
287 transcripts corresponding to the predicted size for *H1R* (403 bp) and *H4R* (353 bp); *H2R* (497 bp)
288 was at the limit of detection. No transcript for *H3R* (221 bp) was detected. Consistent results were
289 obtained when protein expression was evaluated by immunocytofluorescence and confocal analysis
290 (Fig. 3b and c). Indeed, H_1R showed a robust staining with a prominent membrane localisation as
291 demonstrated by its colocalisation with CellMask™ plasma membrane stain (Pearson's coefficient,
292 $r = 0.62$; Mander's coefficients threshold for channel 1, red staining, $tM1 = 0.38$ and Mander's
293 coefficients threshold for channel 2, green staining, $tM2 = 0.93$); moreover, H_1R coimmunolabelling
294 with calnexin ($r = 0.59$; $tM1 = 0.76$ and $tM2 = 0.59$), suggestive of the presence of a proportion of
295 H_1R on the ER, was also revealed. In comparison, H_4R immunolabeling showed a lower
296 immunopositivity level, predominantly within the cytoplasm where a partial positivity was found in
297 the ER ($r = 0.21$, $tM1 = 0.30$ and $tM1 = 0.22$ for the colocalization within the membrane and $r =$
298 0.29 , $tM1 = 0.28$ and $tM2 = 0.33$ for the colocalization within the ER; Fig.3b and c). Very modest,
299 if any, membrane colocalisation was revealed. The staining for H_2R was at the limit of the detection
300 and was not possible to localise it within the membrane.



301

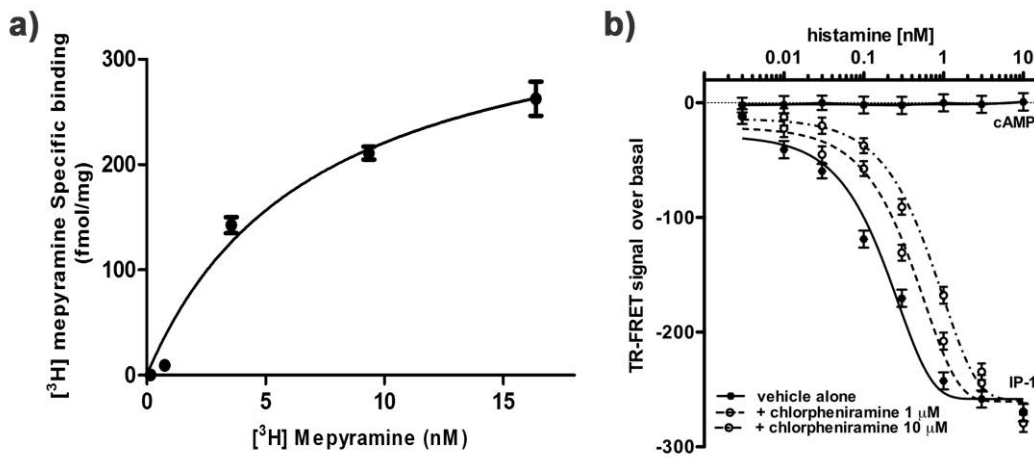
302 **Fig. 3 Histamine receptor expression in human immortalized podocytes.** (a) Agarose gels
 303 representative of 5 independent RT-PCR assays for cDNA from human immortalized podocyte.
 304 Single transcripts corresponding to the size predicted for *H1R* (403 bp), *H2R* (497 bp), *H3R* (221
 305 bp), and *H4R* (353 bp) were detected. The housekeeping gene *GAPDH* was used as control. (b)
 306 Representative merged immunofluorescence images from 5 independent experiments where cells
 307 were labelled with specific anti-H₁ anti-H₂, anti-H₃, or anti-H₄ receptor antibodies (green),

308 respectively, calnexin or CellMask™ Plasma Membrane Stains (red). Nuclei were stained with
309 Hoescht (blue). Detection of yellow colouration, shown by arrows, indicates colocalization. All the
310 slides were examined at $\times 63$ magnification using the SP5 Confocal Laser Scanning Microscope
311 SMD (Leica). (c) Scatterplot of red and green pixel intensities of the maximum projection of the
312 image volume in (b).

313

314 These data suggested the presence of H₁R on the surface of human podocytes, therefore a saturation
315 binding study with the H₁R antagonist mepyramine were performed to quantify the receptor levels.
316 The saturation isotherms revealed a K_d for [³H] mepyramine of 7.02 ± 1.76 nM, indicating the
317 presence of a single class of high affinity binding sites in podocyte membranes. The binding was
318 saturable with a B_{max} estimate of 376 ± 39 fmol/mg protein (Fig. 4a).

319 To further confirm our findings, we tested the activation of the histamine receptors evaluating the
320 levels of cAMP and IP₃ second messengers evoked by histamine. As shown in Fig. 4b, podocytes
321 challenged with histamine (3 pM-10 nM) did not show any changes in cAMP levels, the second
322 messenger predominantly coupled with G_s (such as H₂R) and with G_i (such as H₃R and H₄R)
323 receptors. Notably, cells exposed for 1 h to histamine 3 pM-10 nM showed a concentration-
324 dependent decrease in TR-FRET signal, indicating a sigmoidal increase of IP₁ (EC₅₀ 0.15 ± 0.03
325 nM). The pre-treatment for 10 min with the selective H₁R antagonist chlorpheniramine maleate at
326 either 1 μ M or 10 μ M shifted rightwards in a parallel fashion the curve evoked by histamine in a
327 dose-dependent manner (chlorpheniramine maleate alone did not affect either cAMP or IP₁
328 production; data not shown). Taken together, these data confirm the functional expression of H₁R
329 on podocyte membrane.



330

331 **Fig. 4 Histamine receptor pharmacological profile in human immortalized podocytes.**

332 Saturation binding curve for [³H]mepyramine binding to podocyte cell membrane homogenates (a).

333 Data are the mean ± SD of 3 separate cell preparations determined in triplicate. (b) The levels of

334 IP₁, downstream metabolite of IP₃, and of cAMP were measured, according to the manufacturer's

335 instruction, by IP-One HTRF® assay kit (Cisbio) or by LANCE Ultra cAMP assay (PerkinElmer),

336 respectively. Human immortalized podocytes were pretreated for 10 min with vehicle alone (black

337 hexagon, solid line for IP₁ and white square solid line for cAMP) or the selective H₁R antagonist,

338 chlorpheniramine maleate 1 μM (white circle, dash line) or 10 μM (white circle, dash-dot line),

339 were exposed to histamine (3 pM – 10 nM). Results, expressed as TR-FRET signal over the basal

340 and represented as best-fit concentration-response curve, are the mean ± SEM of 5 independent

341 experiments run in duplicate.

342

343 **3.3 Histamine affects SD protein expression in human immortalized podocyte**

344 The effect evoked by histamine on SD associated proteins ZO-1 and P-cadherin was evaluated at

345 both gene and protein levels. As shown in Fig. 5a and Fig. 6a, cells challenged with histamine (1

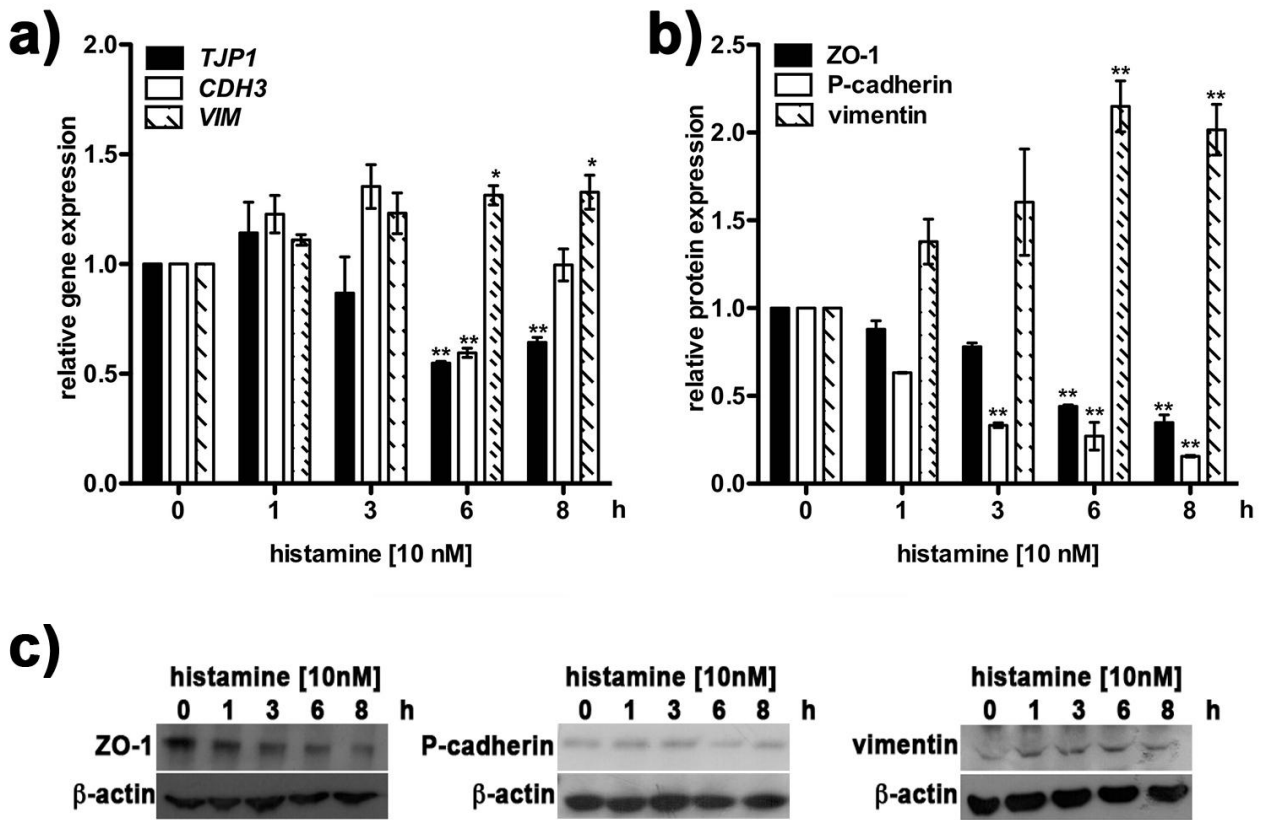
346 pM–10 nM up to 8 h) showed a time- and concentration-dependent reduction of both TJP1, the gene

347 encoding for ZO-1, and CDH3, the encoding gene for P-cadherin, with a maximum of approx. 50%

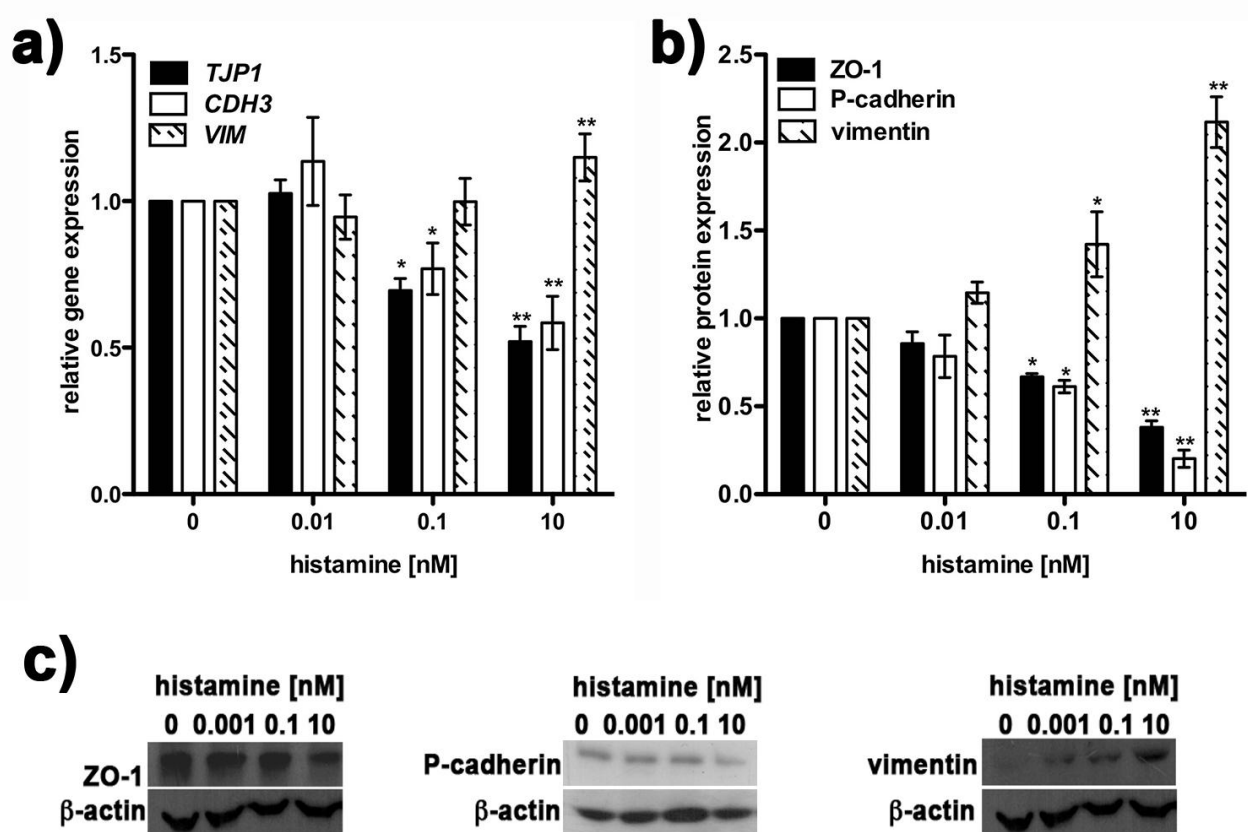
348 after 6 h. Consistently, similar results with a maximum effect at 8 h were obtained when protein

349 expression was evaluated (Fig. 5b and c, and Fig. 6b and c). Moreover, histamine evoked a parallel

350 induction of the intermediate filament vimentin expression (Figure 5a, b and c and Figure 6a, b and
 351 c), a mesenchymal marker associated with podocyte effacement and detachment [40].



352
 353 **Fig. 5 Effect evoked by histamine on ZO-1, P-cadherin and vimentin expression: time-course.**
 354 Effect evoked by histamine on ZO-1, P-cadherin and vimentin expression: time-course. Human
 355 immortalized podocytes were treated with histamine (10 nM) from 0 to 8 h. At selected time *TJP1*,
 356 *CDH3* and *VIM* expression was evaluated by qRT-PCR (a) and ZO-1, P-cadherin and vimentin
 357 protein expression was determined by Western blot analysis (b); results are expressed as mean ±
 358 SEM of five independent experiments; * $P < 0.05$ versus time 0. Pictures shown are representative of
 359 five independent immunoblotting experiments (c).



360

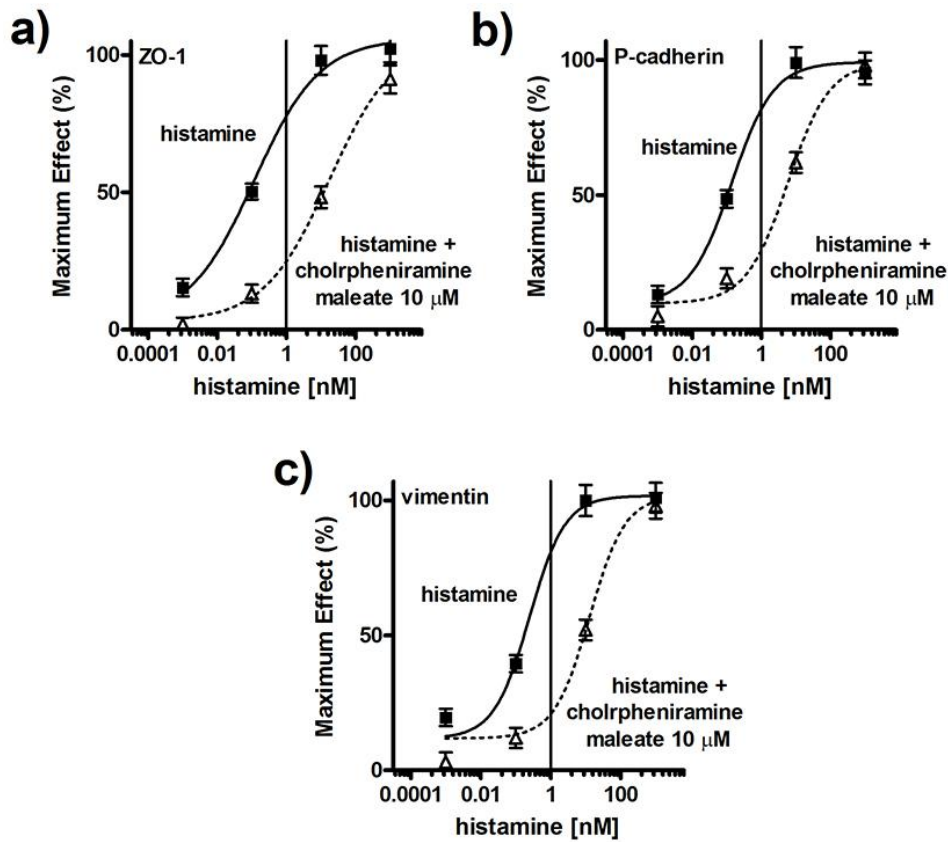
361 **Fig. 6 Effect evoked by histamine on ZO-1, P-cadherin and vimentin expression:**
 362 **concentration-response.** Human immortalized podocytes were treated with histamine (0-10 nM)
 363 for 6 or 8 h and processed for TJP1, CDH3 and VIM expression by qPCR (a) and ZO-1, P-cadherin
 364 and vimentin protein expression by Western blot analysis (b), respectively; results are expressed as
 365 mean ± SEM of five independent experiments, **P* < 0.05 versus 0 (vehicle alone). Pictures shown
 366 are representative of five immunoblotting independent experiments (c).

367

368 Notably, in our experimental condition, synaptopodin and podocin expression, both markers of
 369 podocyte differentiation, was not affected (Supplementary Material Fig. 2)

370 When cells were pre-treated with the selective antagonists chlorpheniramine maleate 10 μM, a
 371 parallel rightward shift of the curves evoked by histamine was observed with an increase in EC₅₀
 372 from 0.09 ± 0.03 nM to 7.62 ± 1.44 nM for ZO-1 (Fig. 7a), from 0.13 ± 0.25 nM to 8.57 ± 2.25 nM

373 for P-cadherin (Fig. 7b) and from 2.40 ± 1.23 nM to 9.76 ± 3.23 nM for vimentin (Fig. 7c),
374 respectively.



375

376 **Fig. 7 Chlorpheniramine antagonism on ZO-1, P-cadherin and vimentin expression evoked by**
377 **histamine.** Human immortalized podocytes pretreated for 10 min with vehicle alone or the
378 selective H₁R antagonist, chlorpheniramine maleate 10 μ M were treated with histamine for 8 h and
379 processed for ZO-1 (a), P-cadherin (b) and vimentin (c) protein expression. Results, represented as
380 best-fit dose-response curve, are expressed as mean \pm SEM of 5 different experiments.

381

382 4 Discussion and Conclusions

383 This study demonstrates for the first time that histamine, via the H₁R, exerts a detrimental direct
384 effect on SD integrity, which results in an increase in podocyte paracellular permeability. This
385 effect is underpinned, in part, by the down-regulation of two key proteins vital for the maintenance
386 of SD integrity, ZO-1 and P-cadherin, with a parallel increase in vimentin expression, the latter
387 probably promoting an epithelial-mesenchymal transition. Interestingly, our study offers, not only a

388 new insight into the effect of histamine on podocyte integrity, but also a clear demonstration of the
389 involvement of histamine in prolonged permeability leakage. Indeed, the extended kinetics of the
390 herein observed events (number of hours) are in keeping and strongly support the delayed
391 mechanism by which histamine increases paracellular permeability involving transcriptional and
392 transductional events [9]. Similar to what was reported for the endothelial junction [41] and in
393 keeping with the ability of histamine to alter adhesion at sites between adjacent cells [42], the
394 results herein suggest that the production of IP₃ by histamine interaction with H₁R triggers the
395 activation of a signalling pathway ultimately resulting in an increase in paracellular permeability.

396 This detrimental effect in the human podocytes is supported by the reduction of the expression of
397 two vital proteins for the SD integrity, ZO-1 and P-cadherin. Notably, although many *in vitro*
398 podocytes cultures showed a cellular dedifferentiation, reflected by loss of processes, and
399 accompanied by a down-regulation of synaptopodyn, our cells displayed a robust mature phenotype
400 as indicated by not only synaptopodin and podocin expression (Supplementary Material Fig. 2a and
401 2c), but also nephrin [43, 44]. Therefore, our *in vitro* system can be considered a suitable new
402 model to study SD-associated proteins. Most notably, our data provide evidence to point to human
403 immortalised podocytes as an interesting new *in vitro* model to study the histaminergic system in
404 naïve human cells. Our *in vitro* cell culture of human immortalised podocytes showed unique
405 expression pattern for both H₁R and HDC enzyme (Supplementary Material Fig. 2a and c), this
406 suggesting that both the autocrine and paracrine effects of this amine could be studied in this
407 system.

408 The unexpected low EC₅₀ (ca. 0.1 nM) herein reported for both ZO-1 and P-cadherin, closely
409 comparable to the one evoked by histamine when IP₃ was measured, could be due, **in part**, to the
410 ability of cells to endogenously produce histamine; indeed, our data show that podocytes clearly
411 express the HDC enzyme (Supplementary Material, Fig. 3 a and b) and that the enzyme is
412 functionally acting, although with a low rate of histamine production (Supplementary Material, Fig.
413 3c). **The atypical apparent high potency of histamine, may also reflect changes in local histamine**

414 concentrations over time, H₁R membrane expression changes and trafficking during the extended
415 exposure period (1-8h), or a large portion of spare receptors. Moreover, splice variations [45] and
416 polymorphisms [46] in human H₁R have been observed, and their eventually occurrence in our cells
417 cannot be ruled out. Although these alternative forms of H₁R have not been pharmacologically
418 characterized thus far, they could be more sensitive to histamine than the wild-type form. The
419 similar shifts in dose-response curves with the racemic (+/-) chlorpheniramine are consistent with
420 the range of published pA₂ values for native H₁R across species and tissues [47-49].

421 Notably, the similar EC₅₀s for ZO-1, P-cadherin and IP₃ led also to speculate that H₁R activation in
422 human podocytes could initiate different and parallel signaling pathways, which converge in the SD
423 dysregulation. For instance, it has been reported that the elevation in IP₃ triggers the protein kinase
424 C activation and evokes calcium efflux from the ER thus promoting signals to the cytoskeleton,
425 ultimately resulting in the increase in permeability [8, 50-52]. However, histamine could affect the
426 cytoskeleton rearrangement through also a phospholipase C-independent mechanism, evoking the
427 phosphorylated myosin light chains accumulation through the RhoA/Rho-associated coiled kinase
428 pathway and activating the mitogen-activated protein kinase p38 [41, 53]. These warrant further
429 investigation.

430 Radioligand binding studies demonstrate high affinity [³H]mepyamine binding sites in the podocyte
431 cells with a mean K_d value comparable to previously published studies for the human H₁R [54].
432 Consistent with functional data indicating that histamine activates only the canonical H₁R-mediated
433 response (second messenger IP₃, evaluated by IP₁), and not H₂R-, H₃R- or H₄R-mediated response
434 (second messenger cAMP), we found that H₁R is predominantly localised on the plasma membrane.
435 Its partial intracellular presence, suggested by co-localization with calnexin, could reflect the
436 receptor trafficking in the presence of nM histamine concentrations.

437 Actually, in human podocytes, we clearly detected the H₄R receptor at both the gene and protein
438 level, although no functional evidence of H₄R were observed. These data raises the discussion of
439 the selectivity of H₄R antibody [55, 56], however we obtained the same results using different

440 commercial H₄R antibodies (Supplementary Material, Fig. 4), at least one of which was validated
441 by H₄R^{-/-} mice. The low level of localisation of the H₄R at the cell membrane could be a possible
442 explanation for the lack of the functional evidence. Indeed, we found a predominantly intracellular
443 localisation accounting for a possible receptor trafficking or for the presence of splice variants of
444 the H₄R. Indeed, the predominant intracellular localisation of H₄R splice variants was already
445 reported by van Rijn and colleagues (2008). However, this speculation needs to be further
446 investigated and also we could not completely rule out the hypothesis that in this cell type, H₄R
447 might activate alternative second messengers, such as the recruitment of β-arrestin [57].

448 Consistent with our results pointing to H₁R as the only histamine receptor functionally expressed in
449 the podocyte membrane, only the pre-treatment with the competitive H₁R antagonist,
450 chlorpheniramine maleate, shifted the curve to the right, while JNJ7777120, a well-known H₄R
451 antagonist prototype, as well as ranitidine, a well-known anti-H₂ antihistamine drug, were both
452 ineffective (Supplementary Material, Fig. 5). All these molecular events, the activation of H₁R
453 leading to the increase in IP₃ production and the co-incident reduction in ZO-1 and P-cadherin, may
454 represent the possible mechanism underlining the detrimental effect of histamine on junction
455 morphological and functional integrity as suggested by the comparable time- and concentration-
456 response profiles. Notably, although P-cadherin protein expression was already affected after 3 h of
457 histamine challenge, the permeability leakage was evident only after 6 h, when also ZO-1
458 expression was reduced. This evidence is in keeping with previous studies showing that modulating
459 P-cadherin alone is not sufficient for the SD dysregulation [58].

460 In addition to ZO-1 and P-cadherin down-regulation a parallel increase of vimentin expression was
461 also observed. Again the concentration-response profile of vimentin induction by histamine was
462 closely comparable to the one evoked by histamine when IP₃ was measured and, again, only the
463 pre-treatment with chlorpheniramine maleate shifted the curve to the right, thus indicating a pure
464 H₁R-mediated event. The increase of mesenchymal markers, such as vimentin, has been associated
465 with podocyte effacement, detachment and loss in diabetic nephropathy [40]. Indeed, podocyte

466 dedifferentiation and mesenchymal transition could be a potential pathway leading to their
467 dysfunction, thereby playing a role in the genesis of proteinuria [59].

468 Histamine was previously demonstrated to alter the link between adherent junction and vimentin in
469 primary human umbilical vein endothelial cells [50]. Moreover, vimentin was also already reported
470 to be upregulated by histamine in primary mouse brain organotypic (MBO) cultures [60]. Vimentin
471 has been also found to be upregulated in podocytes in puromycin aminonucleoside nephrosis [61], a
472 model characterized by the presence of high levels of histamine in the renal cortex, whose abnormal
473 metabolism was postulated to be related both as a cause or a consequence of the pathogenesis
474 [21].

475 Interestingly, until now histamine was assumed only to affect the K_f through the H_1R and H_2R
476 present on mesangial cells, in keeping with the theory that contraction of these cells leads to a
477 reduction in the glomerular capillary surface area. We provide for the first time, molecular
478 pharmacological evidence for a direct effect of histamine on human podocytes, suggestive of a
479 possible use of antihistamines as add-on therapy to counteract the onset and progression of both
480 albuminuria and glomerulosclerosis in different renal aetiologies. Previously, this hypothesis was
481 dismissed by the report that histamine and diphenhydramine had no effect on the alterations in
482 glomerular ultrafiltration that occurs shortly after administration of anti-glomerular basement
483 membrane antibody [62] in a model of acute glomerular immune injury in the rat. However, the
484 authors claimed that it was unlikely that later events would differ greatly regarding a role for
485 histamine because of the effects of locally injected histamine are immediate and should be evident
486 early. In our study, we clearly demonstrate that exposure to low concentrations of histamine
487 promotes important later events on the SD and that these could be prevented by chlorpheniramine.

488 Taken together these data are suggestive of a combined pathophysiological mechanism of histamine
489 on K_f , it evokes not only the mesangial cell contraction but also may promote delayed podocyte
490 detachment, the loss of SD integrity, and subsequent proteinuria and eventual renal damage.

491

492 **Acknowledgements**

493 This work was funded by the Ateneo/CSP2012 (H4 Histamine Receptor As A New
494 Pharmacological Target For The Treatment Of Diabetic Nephropathy - HISDIAN), University of
495 Turin (ex60% 2013), University of Florence (ex60% 2014), and Wolfson Research Institute,
496 Durham University; a preliminary report of this study was presented at the *Queen Elizabeth II*
497 *Conference Centre London Pharmacology 2014, London, UK December 16-18, 2014* and at the *44th*
498 *Annual Meeting of the European Histamine Research Society (EHRS), Malaga, Spain, May 6-9,*
499 *2014*, whose abstract have been published on *Inflammation Research 2015 July; 64 (Suppl1)*. The
500 authors wish to thank Professor Rob Leurs for his kind gift of [³H] mepyramine. **PL Chazot would**
501 **like to dedicate this paper to the memory of his mother.**

502 Authorship contributions is listed as follow: AC Rosa, E Veglia, A Pini and PL Chazot participated
503 in research design; AC Rosa, E Veglia, A Pini, A Moggio, PL Chazot, K Tiligada, C Grange
504 conducted the experiments; F Premoselli has contributed to data acquisition; AC Rosa, E Veglia
505 and A Pini analysed the data; AC Rosa, A Pini, R Fantozzi, G Miglio and PL Chazot wrote or
506 contributed to the writing of the manuscript. All co-authors contributed and have approved the
507 submitted version of the paper.

508

509 **Conflicts of Interest**

510 None

511

512 **References**

513 [1] G. Majno, S.M. Shea, M. Leventhal, Endothelial contraction induced by histamine-type
514 mediators: an electron microscopic study, *The Journal of cell biology* 42(3) (1969) 647-72.

515 [2] J.J. Killackey, M.G. Johnston, H.Z. Movat, Increased permeability of microcarrier-cultured
516 endothelial monolayers in response to histamine and thrombin. A model for the in vitro study of
517 increased vasopermeability, *The American journal of pathology* 122(1) (1986) 50-61.

518 [3] D. Rotrosen, J.I. Gallin, Histamine type I receptor occupancy increases endothelial cytosolic
519 calcium, reduces F-actin, and promotes albumin diffusion across cultured endothelial monolayers,
520 *The Journal of cell biology* 103(6 Pt 1) (1986) 2379-87.

521 [4] K.K. Hamilton, P.J. Sims, Changes in cytosolic Ca²⁺ associated with von Willebrand factor
522 release in human endothelial cells exposed to histamine. Study of microcarrier cell monolayers
523 using the fluorescent probe indo-1, *The Journal of clinical investigation* 79(2) (1987) 600-8.

524 [5] T.A. Brock, E.A. Capasso, Thrombin and histamine activate phospholipase C in human
525 endothelial cells via a phorbol ester-sensitive pathway, *Journal of cellular physiology* 136(1) (1988)
526 54-62.

527 [6] M.R. Carson, S.S. Shasby, D.M. Shasby, Histamine and inositol phosphate accumulation in
528 endothelium: cAMP and a G protein, *The American journal of physiology* 257(4 Pt 1) (1989) L259-
529 64.

530 [7] N. Niimi, N. Noso, S. Yamamoto, The effect of histamine on cultured endothelial cells. A study
531 of the mechanism of increased vascular permeability, *European journal of pharmacology* 221(2-3)
532 (1992) 325-31.

533 [8] T.W. Gardner, T. Leshner, S. Khin, C. Vu, A.J. Barber, W.A. Brennan, Jr., Histamine reduces
534 ZO-1 tight-junction protein expression in cultured retinal microvascular endothelial cells, *The*
535 *Biochemical journal* 320 (Pt 3) (1996) 717-21.

536 [9] K. Takeuchi, C. Kishioka, H. Ishinaga, Y. Sakakura, Y. Majima, Histamine alters gene
537 expression in cultured human nasal epithelial cells, *The Journal of allergy and clinical immunology*
538 107(2) (2001) 310-4.

539 [10] H. Pavenstadt, W. Kriz, M. Kretzler, Cell biology of the glomerular podocyte, *Physiological*
540 *reviews* 83(1) (2003) 253-307.

- 541 [11] I. Ichikawa, B.M. Brenner, Mechanisms of action of hisamine and histamine antagonists on the
542 glomerular microcirculation in the rat, *Circulation research* 45(6) (1979) 737-45.
- 543 [12] D.B. Lee, E. Huang, H.J. Ward, Tight junction biology and kidney dysfunction, *American*
544 *journal of physiology. Renal physiology* 290(1) (2006) F20-34.
- 545 [13] E. Schnabel, J.M. Anderson, M.G. Farquhar, The tight junction protein ZO-1 is concentrated
546 along slit diaphragms of the glomerular epithelium, *The Journal of cell biology* 111(3) (1990) 1255-
547 63.
- 548 [14] D.B. Johnstone, L.B. Holzman, Clinical impact of research on the podocyte slit diaphragm,
549 *Nature clinical practice. Nephrology* 2(5) (2006) 271-82.
- 550 [15] K. Tryggvason, J. Patrakka, Thin basement membrane nephropathy, *Journal of the American*
551 *Society of Nephrology : JASN* 17(3) (2006) 813-22.
- 552 [16] R. Verma, I. Kovari, A. Soofi, D. Nihalani, K. Patrie, L.B. Holzman, Nephrin ectodomain
553 engagement results in Src kinase activation, nephrin phosphorylation, Nck recruitment, and actin
554 polymerization, *The Journal of clinical investigation* 116(5) (2006) 1346-59.
- 555 [17] E. Yaoita, N. Sato, Y. Yoshida, M. Nameta, T. Yamamoto, Cadherin and catenin staining in
556 podocytes in development and puromycin aminonucleoside nephrosis, *Nephrology, dialysis,*
557 *transplantation : official publication of the European Dialysis and Transplant Association -*
558 *European Renal Association* 17 Suppl 9 (2002) 16-9.
- 559 [18] L.N. Sun, Z.X. Chen, X.C. Liu, H.Y. Liu, G.J. Guan, G. Liu, Curcumin ameliorates epithelial-
560 to-mesenchymal transition of podocytes in vivo and in vitro via regulating caveolin-1, *Biomedicine*
561 *& pharmacotherapy = Biomedecine & pharmacotherapie* 68(8) (2014) 1079-88.
- 562 [19] S.J. Shankland, J.W. Pippin, J. Reiser, P. Mundel, Podocytes in culture: past, present, and
563 future, *Kidney international* 72(1) (2007) 26-36.
- 564 [20] P.T. Brinkkoetter, C. Ising, T. Benzing, The role of the podocyte in albumin filtration, *Nature*
565 *reviews. Nephrology* 9(6) (2013) 328-36.

566 [21] H.E. Abboud, S.L. Ou, J.A. Velosa, S.V. Shah, T.P. Dousa, Dynamics of renal histamine in
567 normal rat kidney and in nephrosis induced by aminonucleoside of puromycin, *The Journal of*
568 *clinical investigation* 69(2) (1982) 327-36.

569 [22] J.R. Sedor, H.E. Abboud, Actions and metabolism of histamine in glomeruli and tubules of the
570 human kidney, *Kidney international* 26(2) (1984) 144-52.

571 [23] J.R. Sedor, H.E. Abboud, Histamine modulates contraction and cyclic nucleotides in cultured
572 rat mesangial cells. Differential effects mediated by histamine H1 and H2 receptors, *The Journal of*
573 *clinical investigation* 75(5) (1985) 1679-89.

574 [24] A.C. Rosa, C. Grange, A. Pini, M.A. Katebe, E. Benetti, M. Collino, G. Miglio, D. Bani, G.
575 Camussi, P.L. Chazot, R. Fantozzi, Overexpression of histamine H(4) receptors in the kidney of
576 diabetic rat, *Inflammation research : official journal of the European Histamine Research Society ...*
577 [et al.] 62(4) (2013) 357-65.

578 [25] A. Pini, P.L. Chazot, E. Veglia, A. Moggio, A.C. Rosa, H3 receptor renal expression in normal
579 and diabetic rats, *Inflammation research : official journal of the European Histamine Research*
580 *Society ... [et al.]* 64(5) (2015) 271-3.

581 [26] E. Veglia, C. Grange, A. Pini, A. Moggio, C. Lanzi, G. Camussi, P.L. Chazot, A.C. Rosa,
582 Histamine receptor expression in human renal tubules: a comparative pharmacological evaluation,
583 *Inflammation research : official journal of the European Histamine Research Society ... [et al.]*
584 64(3-4) (2015) 261-70.

585 [27] P.G. Conaldi, L. Biancone, A. Bottelli, A. De Martino, G. Camussi, A. Toniolo, Distinct
586 pathogenic effects of group B coxsackieviruses on human glomerular and tubular kidney cells,
587 *Journal of virology* 71(12) (1997) 9180-7.

588 [28] S. Doublier, V. Ruotsalainen, G. Salvidio, E. Lupia, L. Biancone, P.G. Conaldi, P. Reponen,
589 K. Tryggvason, G. Camussi, Nephric redistribution on podocytes is a potential mechanism for
590 proteinuria in patients with primary acquired nephrotic syndrome, *The American journal of*
591 *pathology* 158(5) (2001) 1723-31.

592 [29] F. Collino, M.C. Deregibus, S. Bruno, L. Sterpone, G. Aghemo, L. Viltono, C. Tetta, G.
593 Camussi, Microvesicles derived from adult human bone marrow and tissue specific mesenchymal
594 stem cells shuttle selected pattern of miRNAs, *PloS one* 5(7) (2010) e11803.

595 [30] A.S. Awad, M. Rouse, L. Liu, A.L. Vergis, D.L. Rosin, J. Linden, J.R. Sedor, M.D. Okusa,
596 Activation of adenosine 2A receptors preserves structure and function of podocytes, *Journal of the*
597 *American Society of Nephrology : JASN* 19(1) (2008) 59-68.

598 [31] M. Dey, A. Baldys, D.B. Sumter, P. Gooz, L.M. Luttrell, J.R. Raymond, M. Gooz, Bradykinin
599 decreases podocyte permeability through ADAM17-dependent epidermal growth factor receptor
600 activation and zonula occludens-1 rearrangement, *The Journal of pharmacology and experimental*
601 *therapeutics* 334(3) (2010) 775-83.

602 [32] A.C. Rosa, L. Rattazzi, G. Miglio, M. Collino, R. Fantozzi, Angiotensin II induces tumor
603 necrosis factor-alpha expression and release from cultured human podocytes, *Inflammation research*
604 *: official journal of the European Histamine Research Society ... [et al.]* 61(4) (2012) 311-7.

605 [33] R.M. van Rijn, P.L. Chazot, F.C. Shenton, K. Sansuk, R.A. Bakker, R. Leurs, Oligomerization
606 of recombinant and endogenously expressed human histamine H(4) receptors, *Mol Pharmacol* 70(2)
607 (2006) 604-15.

608 [34] D. Dijkstra, R. Leurs, P. Chazot, F.C. Shenton, H. Stark, T. Werfel, R. Gutzmer, Histamine
609 downregulates monocyte CCL2 production through the histamine H4 receptor, *The Journal of*
610 *allergy and clinical immunology* 120(2) (2007) 300-7.

611 [35] W. Baumer, S. Wendorff, R. Gutzmer, T. Werfel, D. Dijkstra, P. Chazot, H. Stark, M.
612 Kietzmann, Histamine H4 receptors modulate dendritic cell migration through skin--
613 immunomodulatory role of histamine, *Allergy* 63(10) (2008) 1387-94.

614 [36] D. Dijkstra, H. Stark, P.L. Chazot, F.C. Shenton, R. Leurs, T. Werfel, R. Gutzmer, Human
615 inflammatory dendritic epidermal cells express a functional histamine H4 receptor, *The Journal of*
616 *investigative dermatology* 128(7) (2008) 1696-703.

617 [37] D. Grandi, F.C. Shenton, P.L. Chazot, G. Morini, Immunolocalization of histamine H3
618 receptors on endocrine cells in the rat gastrointestinal tract, *Histology and histopathology* 23(7)
619 (2008) 789-98.

620 [38] G. Morini, G. Becchi, F.C. Shenton, P.L. Chazot, D. Grandi, Histamine H3 and H4 receptors
621 are expressed on distinct endocrine cell types in the rat fundic mucosa, *Inflammation research :
622 official journal of the European Histamine Research Society ... [et al.]* 57 Suppl 1 (2008) S57-8.

623 [39] R.M. van Rijn, A. van Marle, P.L. Chazot, E. Langemeijer, Y. Qin, F.C. Shenton, H.D. Lim,
624 O.P. Zuiderveld, K. Sansuk, M. Dy, M.J. Smit, C.P. Tensen, R.A. Bakker, R. Leurs, Cloning and
625 characterization of dominant negative splice variants of the human histamine H4 receptor, *The
626 Biochemical journal* 414(1) (2008) 121-31.

627 [40] K. Reidy, K. Susztak, Epithelial-mesenchymal transition and podocyte loss in diabetic kidney
628 disease, *American journal of kidney diseases : the official journal of the National Kidney
629 Foundation* 54(4) (2009) 590-3.

630 [41] S.P. Adderley, X.E. Zhang, J.W. Breslin, Involvement of the H1 histamine receptor, p38 MAP
631 kinase, MLCK, and Rho/ROCK in histamine-induced endothelial barrier dysfunction,
632 *Microcirculation* (2015).

633 [42] Q. Zhang, K. Fisher, Tight junction-related barrier contributes to the electrophysiological
634 asymmetry across vocal fold epithelium, *PloS one* 7(3) (2012) e34017.

635 [43] G. Miglio, A.C. Rosa, L. Rattazzi, C. Grange, M. Collino, G. Camussi, R. Fantozzi, The
636 subtypes of peroxisome proliferator-activated receptors expressed by human podocytes and their
637 role in decreasing podocyte injury, *British journal of pharmacology* 162(1) (2011) 111-25.

638 [44] G. Miglio, A.C. Rosa, L. Rattazzi, C. Grange, G. Camussi, R. Fantozzi, Protective effects of
639 peroxisome proliferator-activated receptor agonists on human podocytes: proposed mechanisms of
640 action, *British journal of pharmacology* 167(3) (2012) 641-53.

641 [45] C. Swan, S.A. Richards, N.P. Duroudier, I. Sayers, I.P. Hall, Alternative promoter use and
642 splice variation in the human histamine H1 receptor gene, *American journal of respiratory cell and*
643 *molecular biology* 35(1) (2006) 118-26.

644 [46] B.R. Godlewska, L. Olajosy-Hilkesberger, M. Olajosy, J. Limon, J. Landowski,
645 Polymorphisms of the histamine receptor (H1HR) gene are not associated with olanzapine-induced
646 weight gain, *Journal of clinical psychopharmacology* 33(3) (2013) 436-7.

647 [47] R. Leurs, M.M. Brozius, M.J. Smit, A. Bast, H. Timmerman, Effects of histamine H1-, H2-
648 and H3-receptor selective drugs on the mechanical activity of guinea-pig small and large intestine,
649 *British journal of pharmacology* 102(1) (1991) 179-85.

650 [48] M. Al-Gadi, S.J. Hill, Characterization of histamine receptors mediating the stimulation of
651 cyclic AMP accumulation in rabbit cerebral cortical slices, *British journal of pharmacology* 85(4)
652 (1985) 877-88.

653 [49] A.N. Nicholson, P.A. Pascoe, C. Turner, C.R. Ganellin, P.M. Greengrass, A.F. Casy, A.D.
654 Mercer, Sedation and histamine H1-receptor antagonism: studies in man with the enantiomers of
655 chlorpheniramine and dimethindene, *British journal of pharmacology* 104(1) (1991) 270-6.

656 [50] D.M. Shasby, D.R. Ries, S.S. Shasby, M.C. Winter, Histamine stimulates phosphorylation of
657 adherens junction proteins and alters their link to vimentin, *American journal of physiology. Lung*
658 *cellular and molecular physiology* 282(6) (2002) L1330-8.

659 [51] R.A. Budworth, M. Anderson, R.H. Clothier, L. Leach, Histamine-induced Changes in the
660 Actin Cytoskeleton of the Human Microvascular Endothelial Cell line HMEC-1, *Toxicology in*
661 *vitro : an international journal published in association with BIBRA* 13(4-5) (1999) 789-95.

662 [52] S.Y. Yuan, Signal transduction pathways in enhanced microvascular permeability,
663 *Microcirculation* 7(6 Pt 1) (2000) 395-403.

664 [53] C.M. Mikelis, M. Simaan, K. Ando, S. Fukuhara, A. Sakurai, P. Amornphimoltham, A.
665 Masedunskas, R. Weigert, T. Chavakis, R.H. Adams, S. Offermanns, N. Mochizuki, Y. Zheng, J.S.

666 Gutkind, RhoA and ROCK mediate histamine-induced vascular leakage and anaphylactic shock,
667 Nature communications 6 (2015) 6725.

668 [54] S. Hishinuma, J.M. Young, Characteristics of the binding of [3H]-mepyramine to intact human
669 U373 MG astrocytoma cells: evidence for histamine-induced H1-receptor internalisation, British
670 journal of pharmacology 116(6) (1995) 2715-23.

671 [55] S. Beermann, R. Seifert, D. Neumann, Commercially available antibodies against human and
672 murine histamine H(4)-receptor lack specificity, Naunyn-Schmiedeberg's archives of pharmacology
673 385(2) (2012) 125-35.

674 [56] R. Gutzmer, T. Werfel, W. Baumer, M. Kietzmann, P.L. Chazot, R. Leurs, Well characterized
675 antihistamine 4 receptor antibodies contribute to current knowledge of the expression and biology
676 of the human and murine histamine 4 receptor, Naunyn-Schmiedeberg's archives of pharmacology
677 385(9) (2012) 853-4; author reply 855-60.

678 [57] R. Seifert, E.H. Schneider, S. Dove, I. Brunskole, D. Neumann, A. Strasser, A. Buschauer,
679 Paradoxical stimulatory effects of the "standard" histamine H4-receptor antagonist JNJ7777120: the
680 H4 receptor joins the club of 7 transmembrane domain receptors exhibiting functional selectivity,
681 Mol Pharmacol 79(4) (2011) 631-8.

682 [58] J. Reiser, W. Kriz, M. Kretzler, P. Mundel, The glomerular slit diaphragm is a modified
683 adherens junction, Journal of the American Society of Nephrology : JASN 11(1) (2000) 1-8.

684 [59] Y. Li, Y.S. Kang, C. Dai, L.P. Kiss, X. Wen, Y. Liu, Epithelial-to-mesenchymal transition is a
685 potential pathway leading to podocyte dysfunction and proteinuria, The American journal of
686 pathology 172(2) (2008) 299-308.

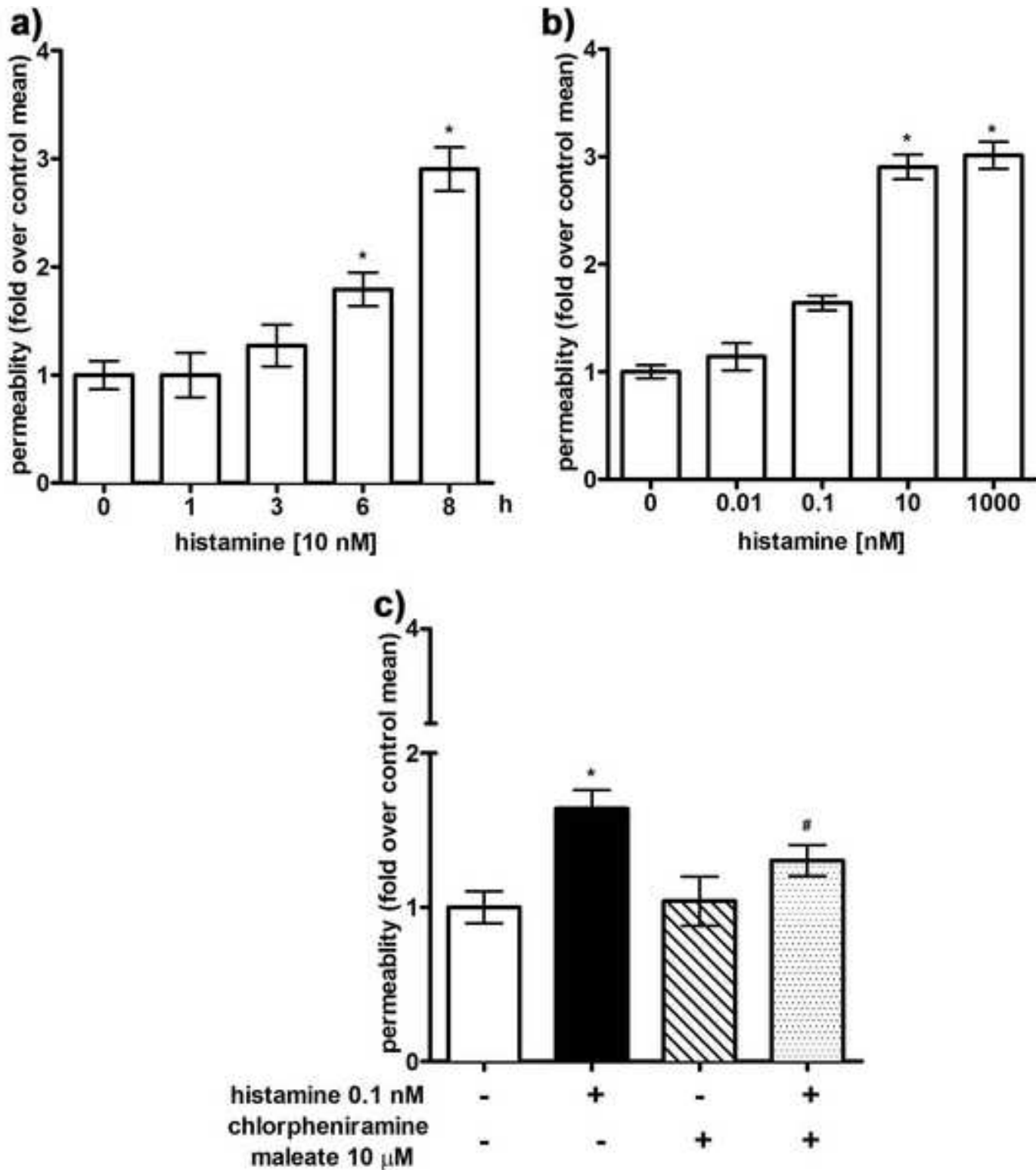
687 [60] J.C. Sedeyn, H. Wu, R.D. Hobbs, E.C. Levin, R.G. Nagele, V. Venkataraman, Histamine
688 Induces Alzheimer's Disease-Like Blood Brain Barrier Breach and Local Cellular Responses in
689 Mouse Brain Organotypic Cultures, BioMed research international 2015 (2015) 937148.

690 [61] J. Zou, E. Yaoita, Y. Watanabe, Y. Yoshida, M. Nameta, H. Li, Z. Qu, T. Yamamoto,
691 Upregulation of nestin, vimentin, and desmin in rat podocytes in response to injury, *Virchows*
692 *Archiv : an international journal of pathology* 448(4) (2006) 485-92.

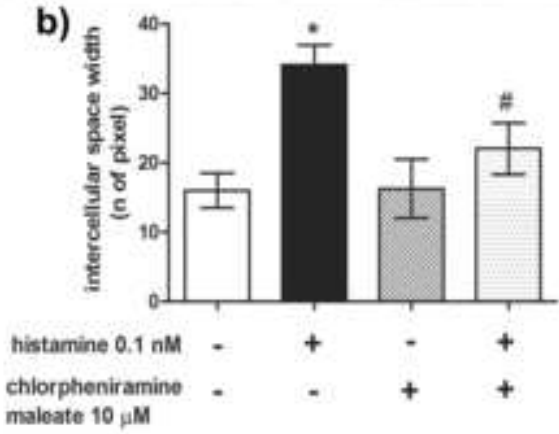
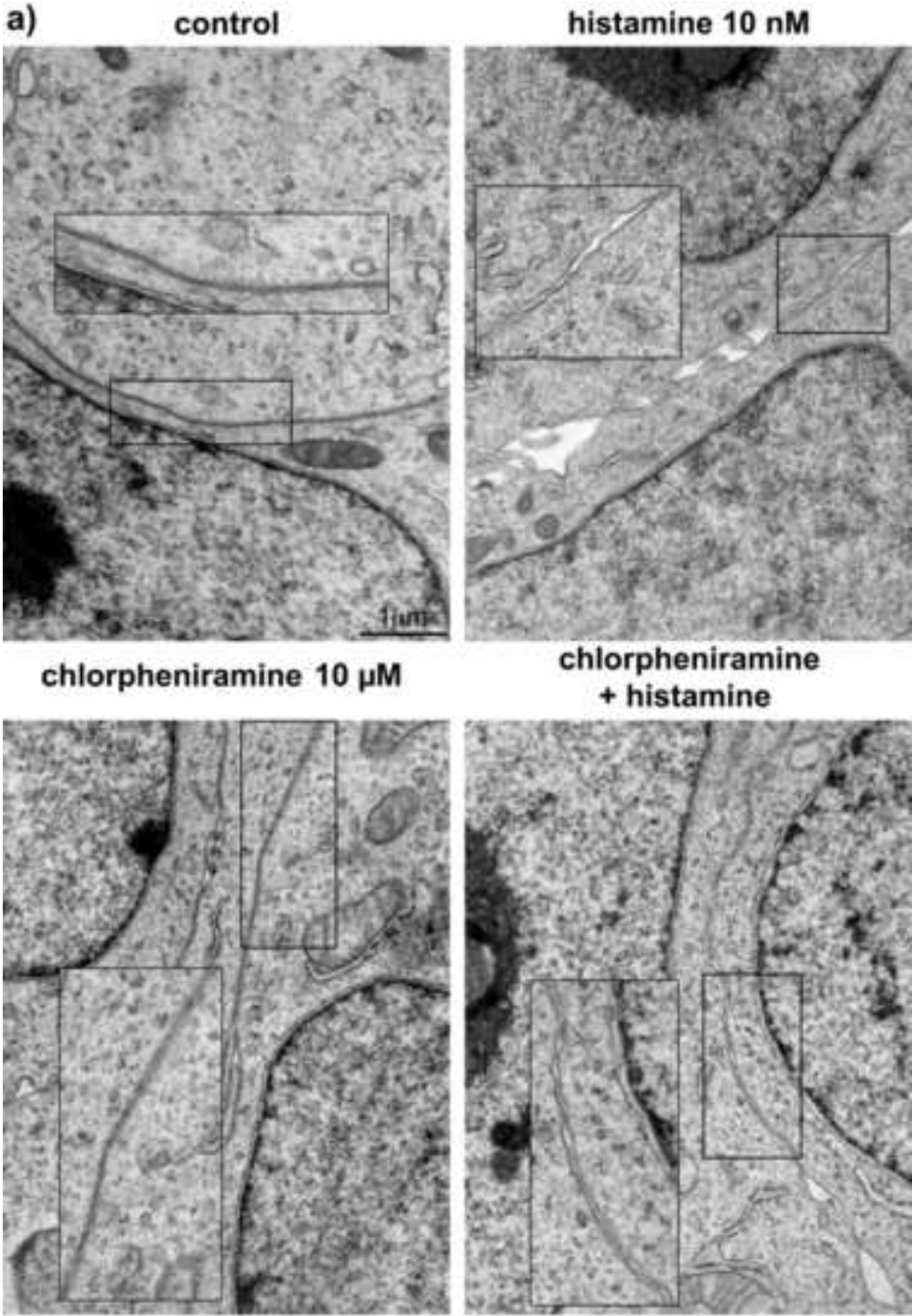
693 [62] C.B. Wilson, L.C. Gushwa, O.W. Peterson, B.J. Tucker, R.C. Blantz, Glomerular immune
694 injury in the rat: effect of antagonists of histamine activity, *Kidney international* 20(5) (1981) 628-
695 35.

696

Figure(s) 1
[Click here to download high resolution image](#)

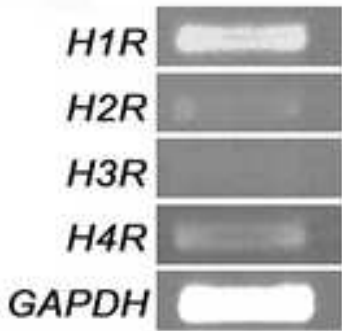


Figure(s) 2
[Click here to download high resolution image](#)

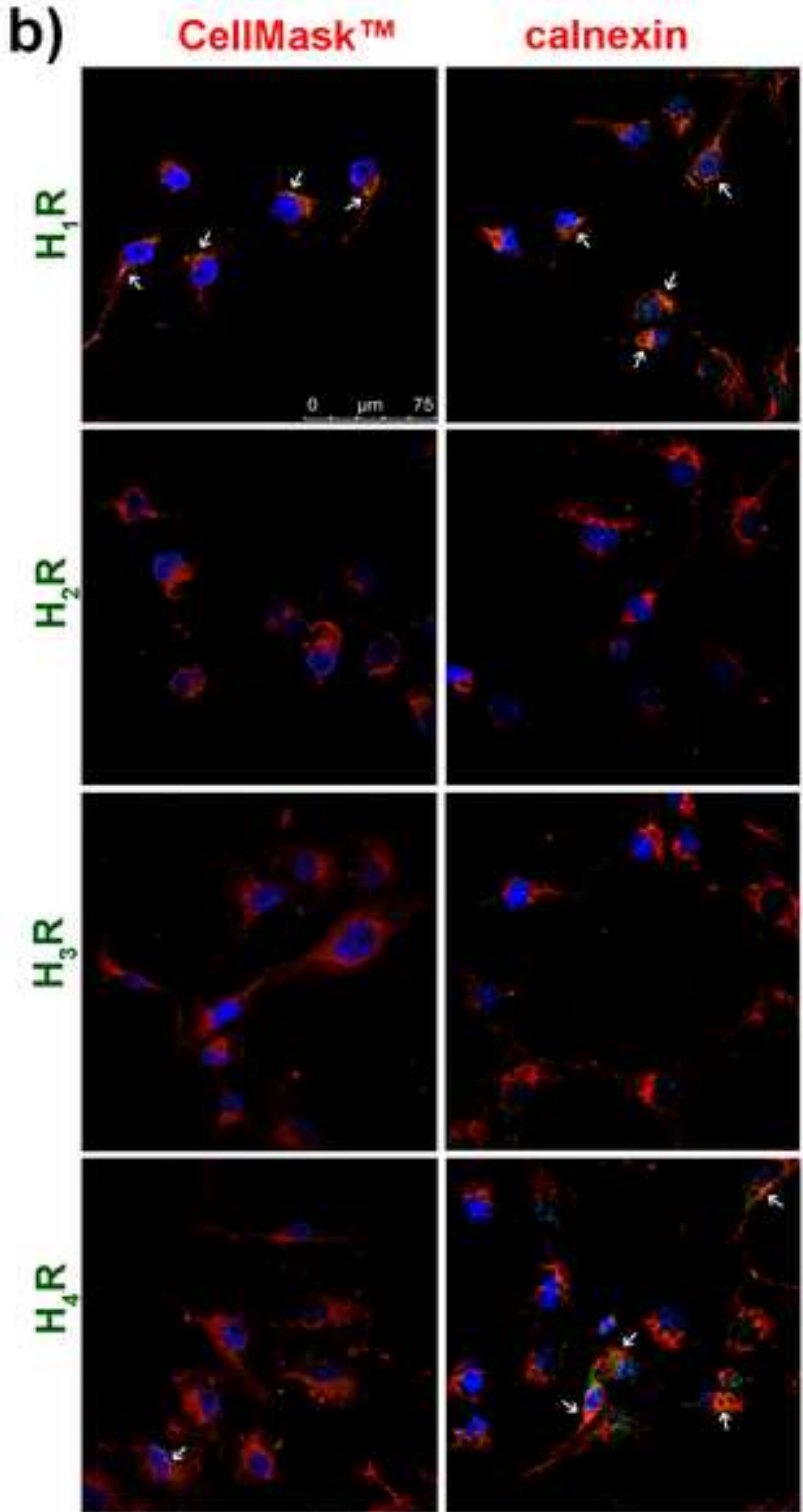


Figure(s) 3
[Click here to download high resolution image](#)

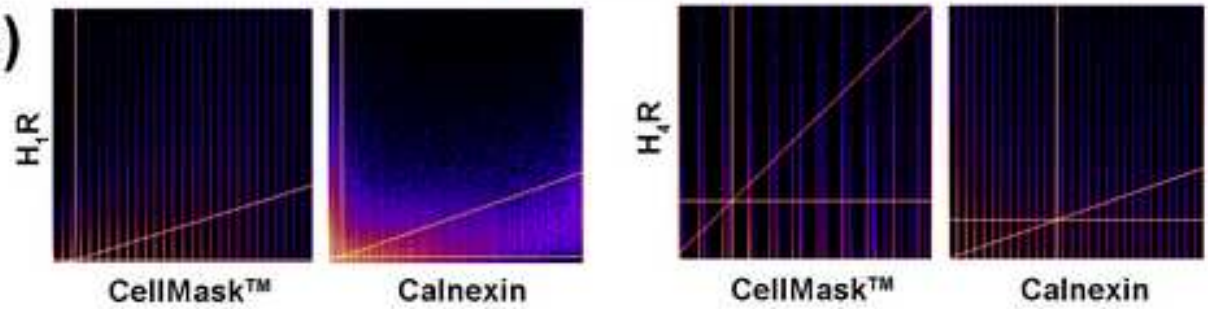
a)

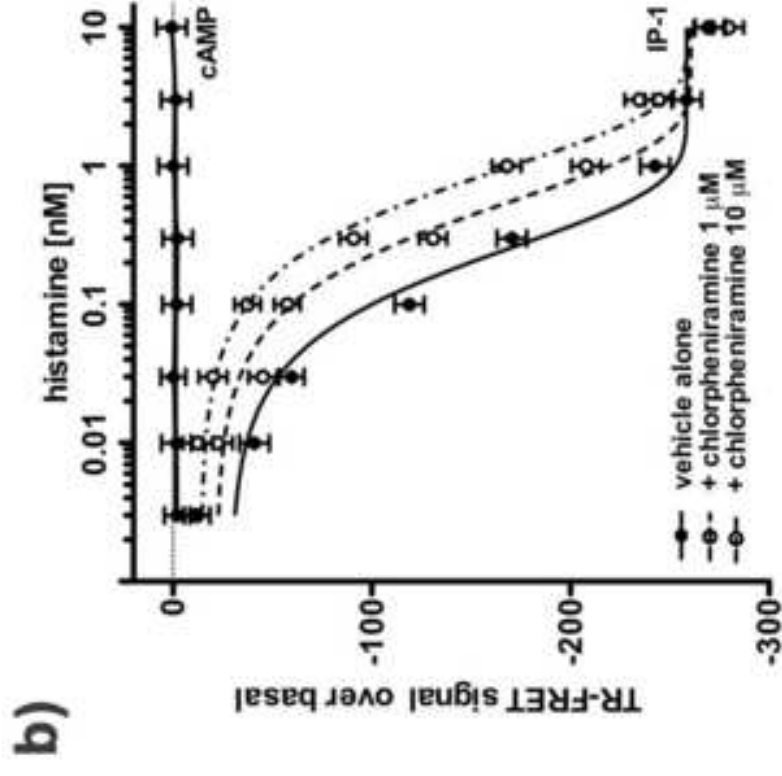
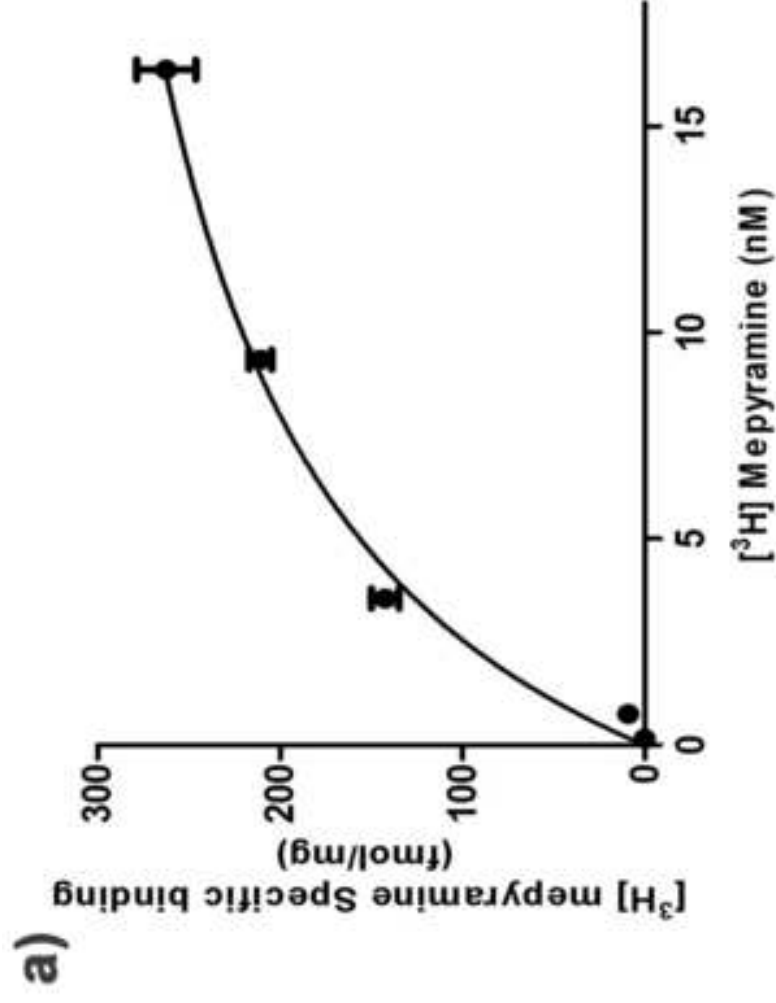


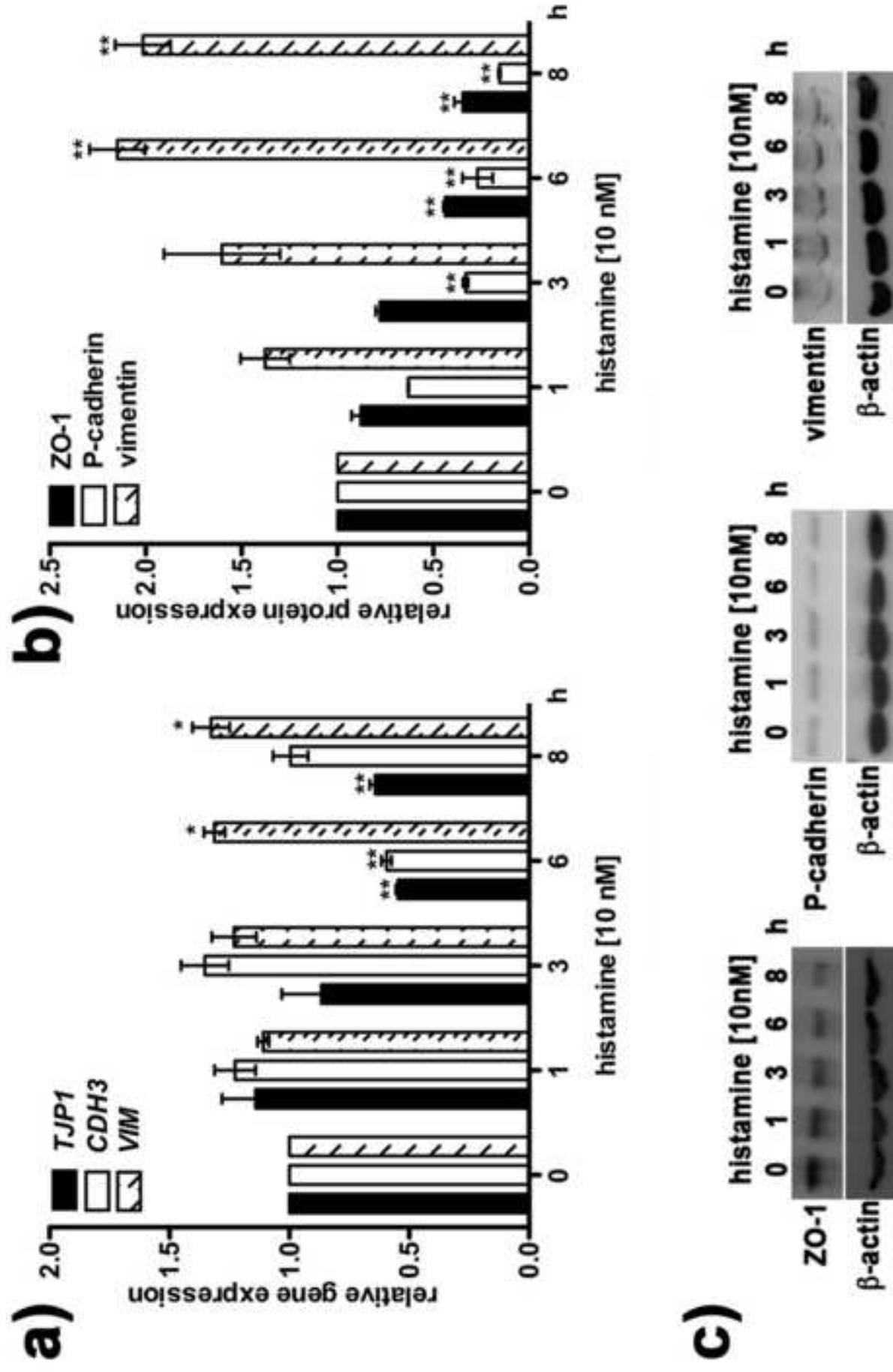
b)

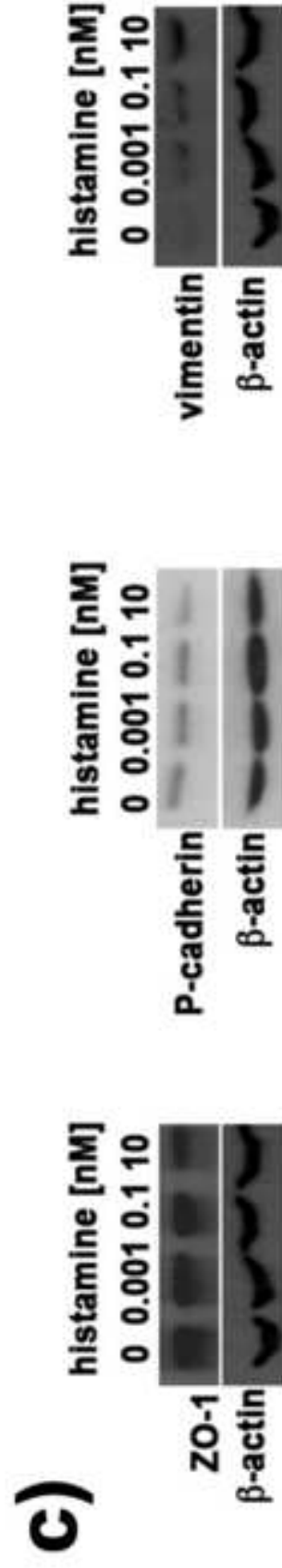
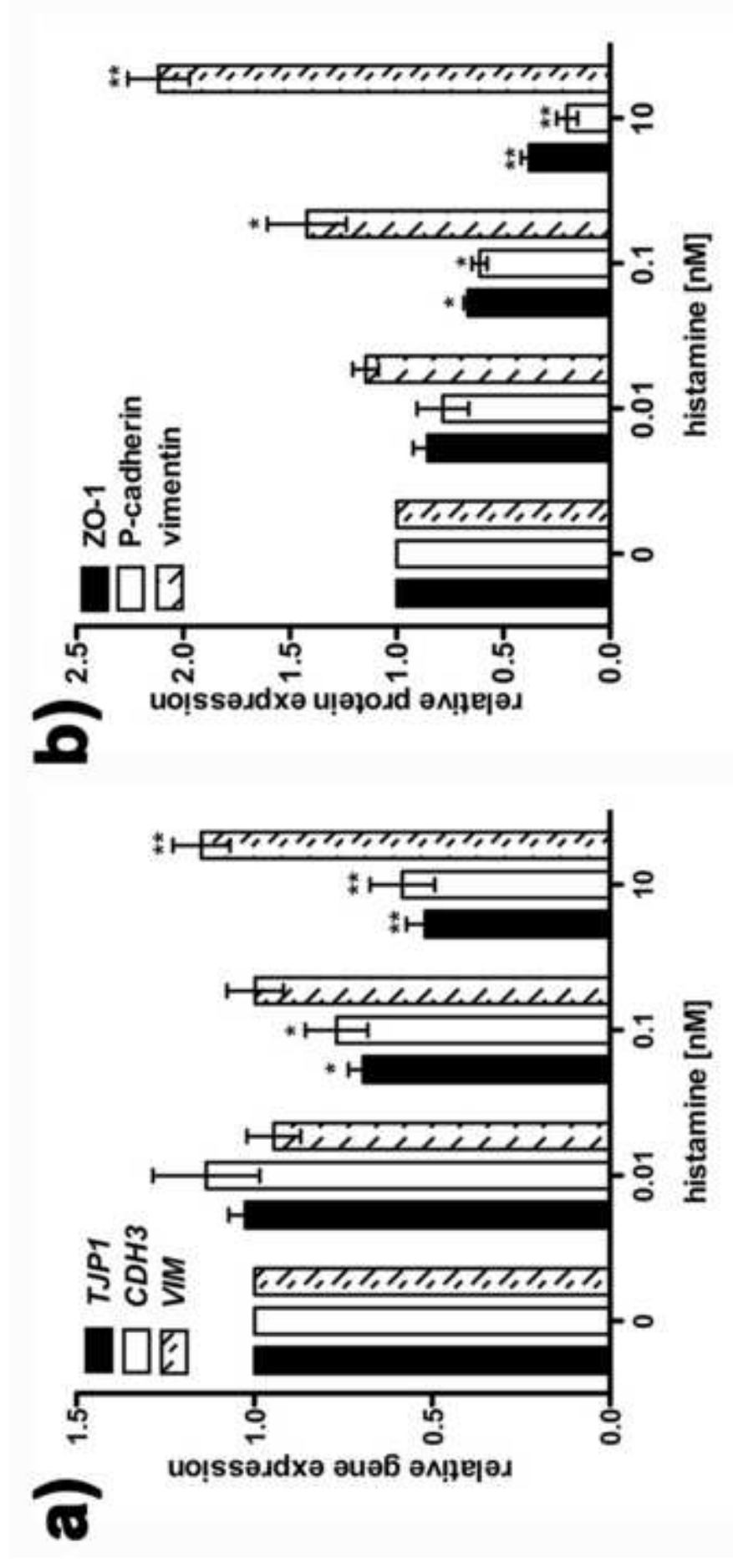


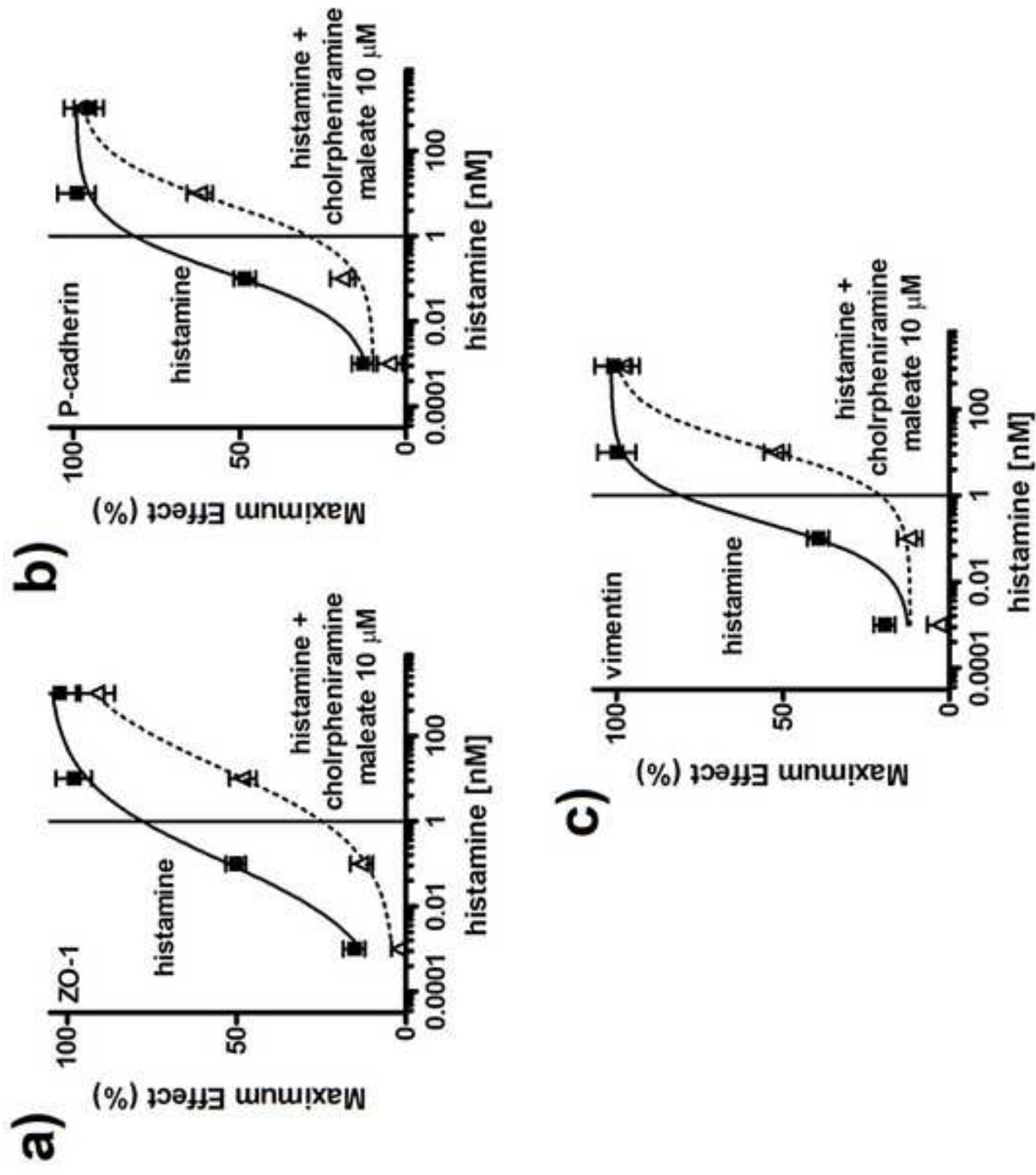
c)











List of chemical compounds studied in the article

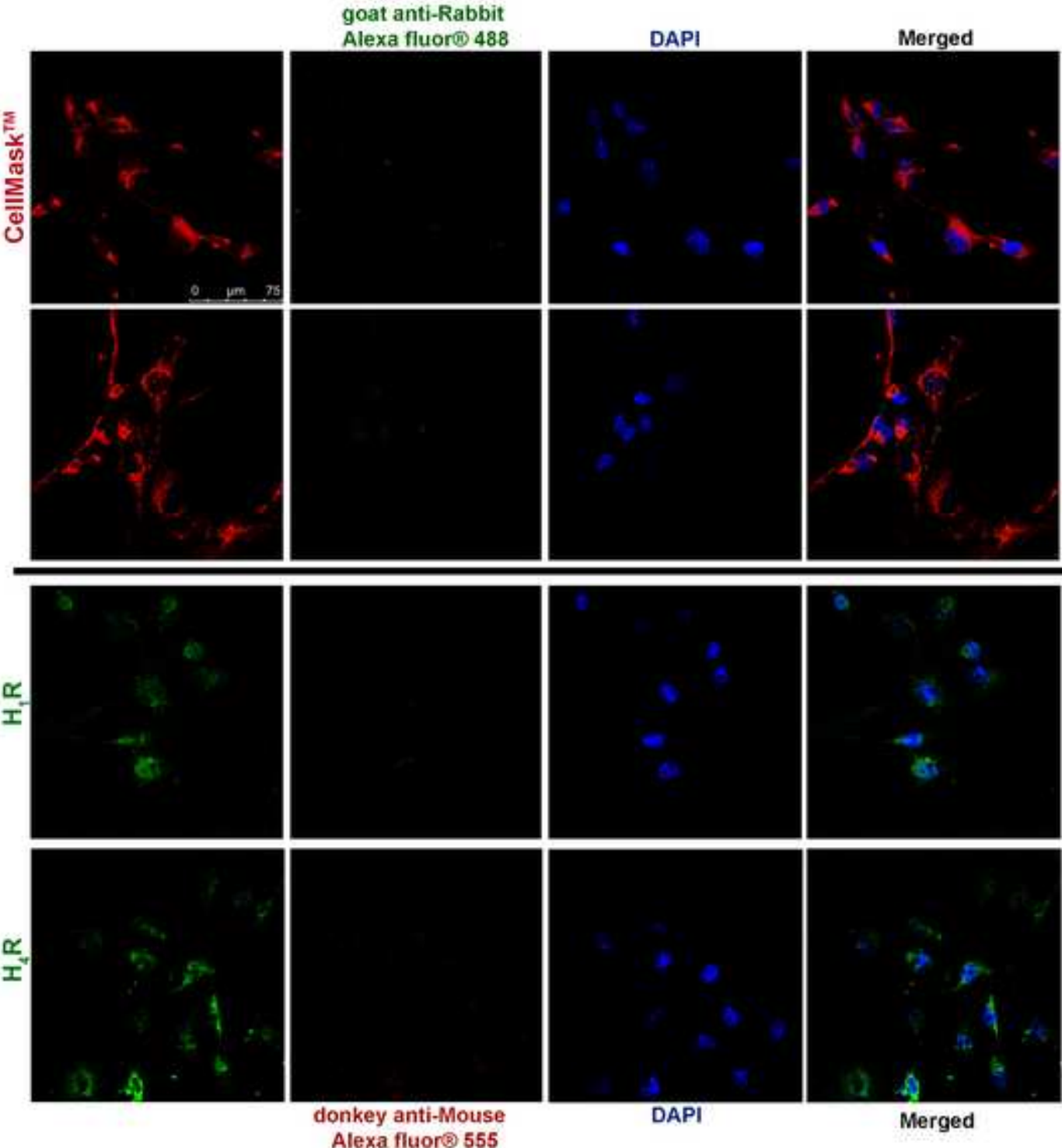
1. [³H]mepyramine PubChem CID 656400
2. Chlorpheniramine maleate PubChem CID 5281068
3. Difenhydramine Pubmed CID 3100
4. Histamine dihydrochloride PubChem CID 5818

Supplementary Material - Materials and Methods***Immunocytofluorescence and confocal analysis***

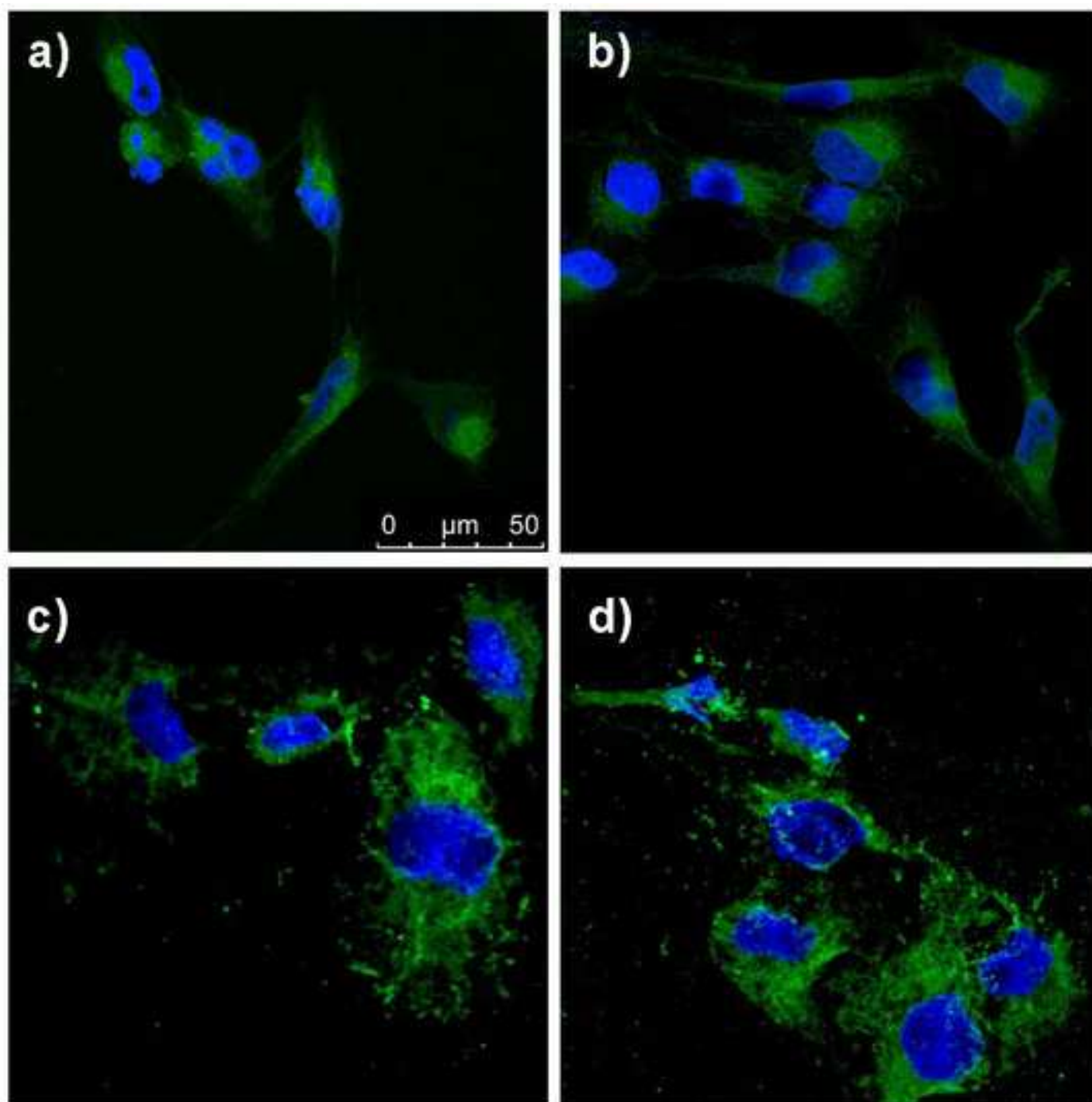
Podocytes plated on collagen-coated cover glasses treated with vehicle alone or histamine 10 nM for 0-8 h, were fixed with 4% paraformaldehyde for 10 minutes at room temperature. Sections were incubated overnight with goat polyclonal anti-synaptopodin 1.3 µg/ml (N14, sc-21536), rabbit anti-podocin 2 µg/ml (H130, sc-21009), goat anti-rabbit H₄R 2 µg/ml (Y19 sc-33967; Santa Cruz Biotechnology Inc., Dallas, TX, USA), or rabbit polyclonal anti-HDC 0.4 µg/ml (HPA038891; Sigma–Aldrich St. Louis, MO) at 4°C. After incubation with the respective Alexa-Conjugated secondary antibodies the nuclei were stained with Hoescht. All the slides were examined at ×63 magnification using the SP5 Confocal Laser Scanning Microscope SMD (Leica). A variable number of optical section images in the z-dimension (z-spacing, 0.42 µm) were collected ensuring that images throughout the 3D cellular structure, spanning multiple confocal planes, were fully captured.

Fluorometric quantification of histamine

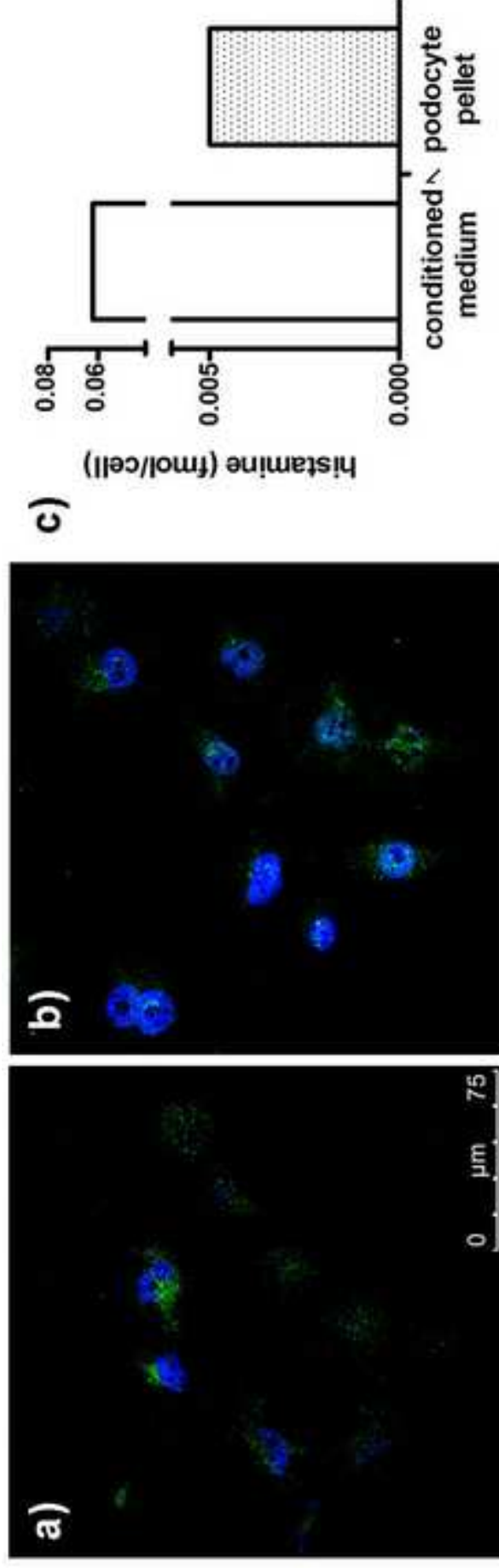
Podocytes seeded at a density of 800.000 cell/ml were pelleted after one hour from medium re-challenge and the medium was collected. Both pellet and medium were processed accordingly to the standard fluorimetric protocol reported in the Histamine Methods & Tools Database (<https://www.i-med.ac.at/hmtd/>) for the quantification of histamine. Histamine extracted in *n*-butanol was reconstituted in aqueous phase using 0.1 N sulphuric acid and *n*-heptane and assayed fluorometrically at 360 nm excitation (Tiligada E, et al. Pharmacol Res 2000).



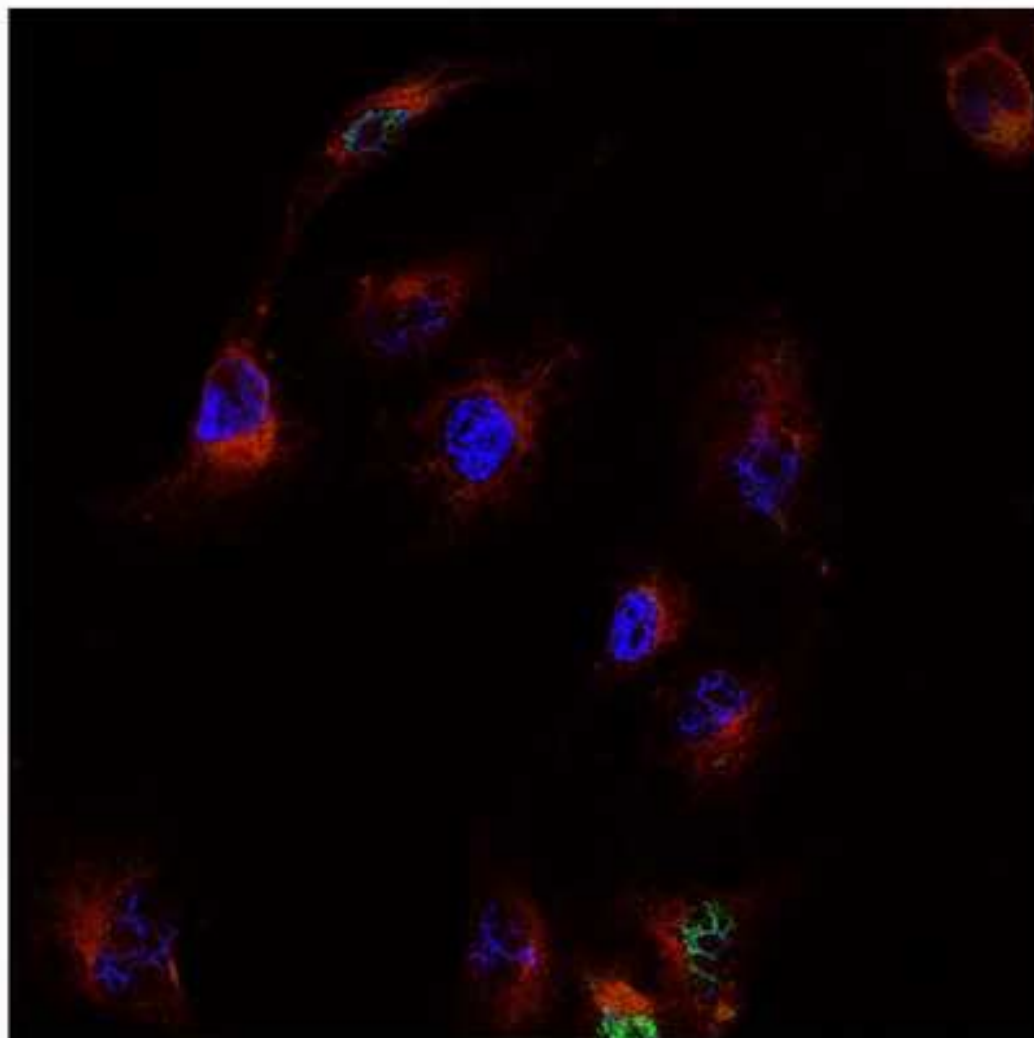
Supplementary Material Fig. 1. Nonspecific binding of the secondary antibodies in colocalization experiments. Representative maximum projection of podocyte Z sections showing the interactions between the different antibodies used. All the slides were examined at $\times 63$ magnification using the SP5 Confocal Laser Scanning Microscope SMD (Leica).



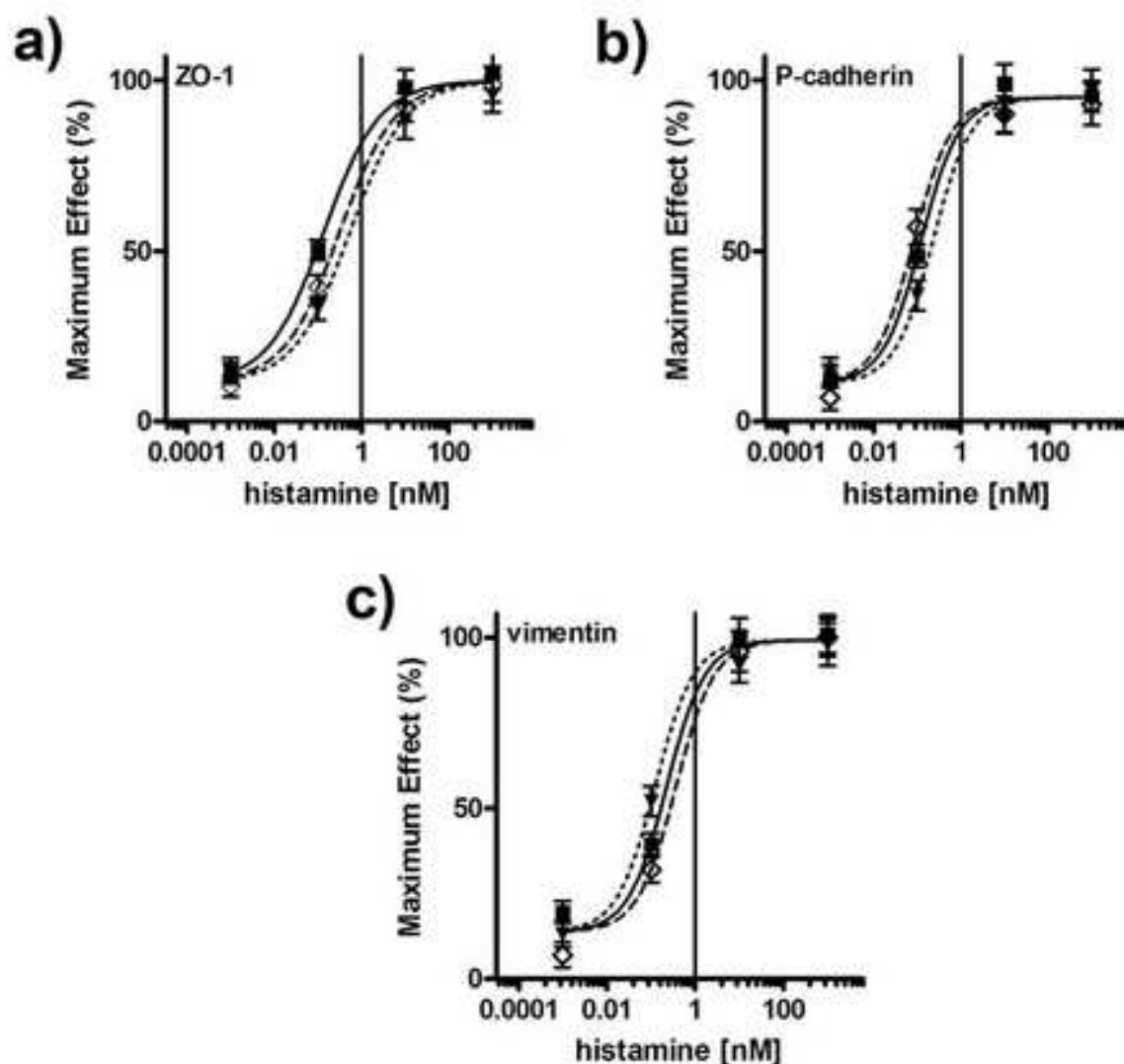
Supplementary Material Fig. 2. Synaptopodin and podocin expression in human immortalized podocytes. Representative maximum projection of the Z sections from 3 independent experiments where cells treated with histamine 10 nM for 0 (a) or 8 (b) h were labelled with specific anti-synaptopodin (a) and (b) or (c) and (d) anti-podocin antibody (green). Nuclei were stained with Hoescht (blue). All the slides were examined at $\times 63$ magnification using the SP5 Confocal Laser Scanning Microscope SMD (Leica).



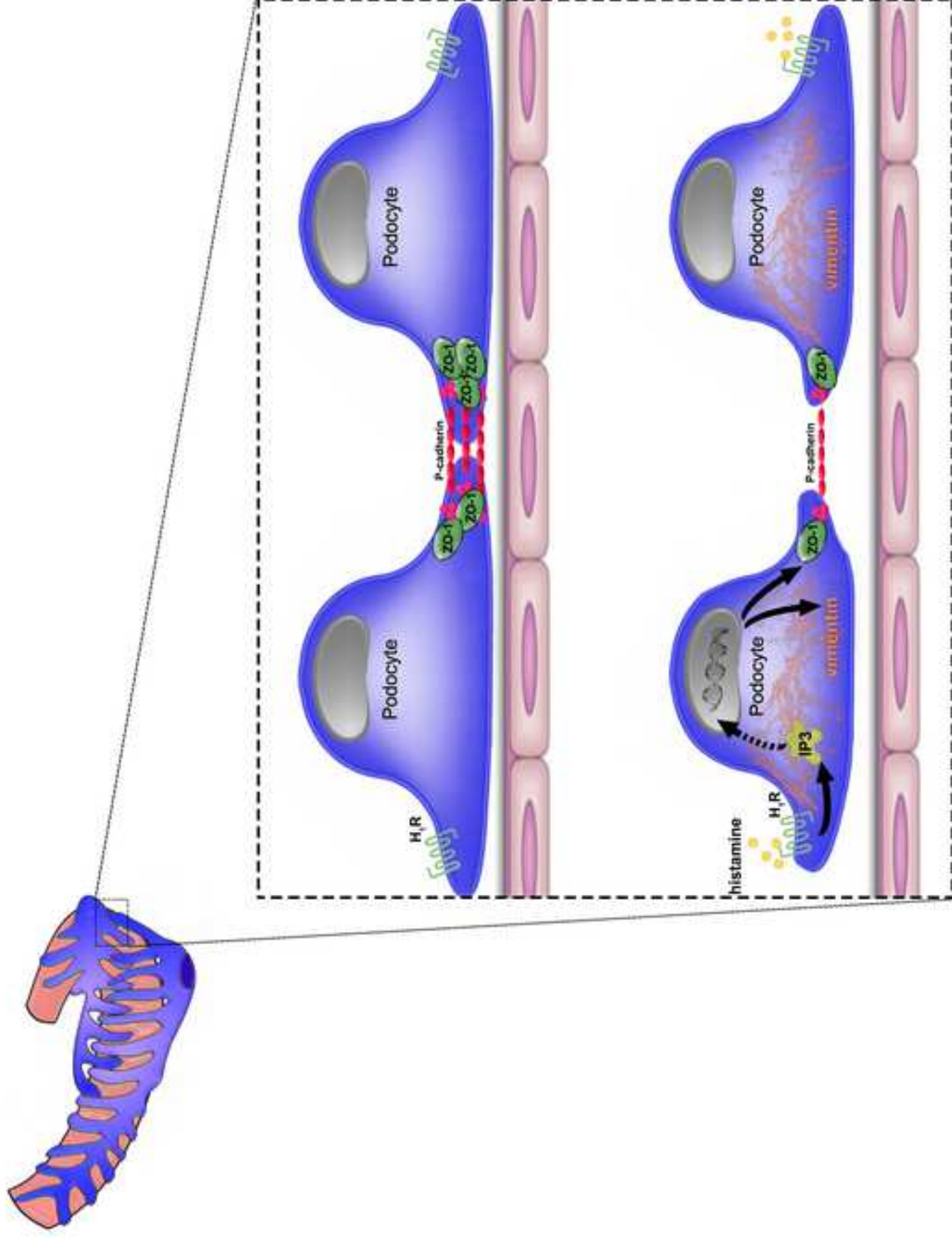
Supplementary Material Fig. 3. HDC expression and histamine production in human immortalized podocytes. Representative maximum projection of the Z sections from 3 independent experiments where cells treated with histamine 10 nM for 0 (a) or 8 (b) h were labelled with the specific anti-HDC antibody (green). Nuclei were stained with Hoescht (blue). All the slides were examined at $\times 63$ magnification using the SP5 Confocal Laser Scanning Microscope SMD (Leica). Histamine basal production was measured in two independent experiments after 1 h of medium rechellenge in both the conditioned medium and the podocyte pellet accordingly to the fluorometric quantification method (c).

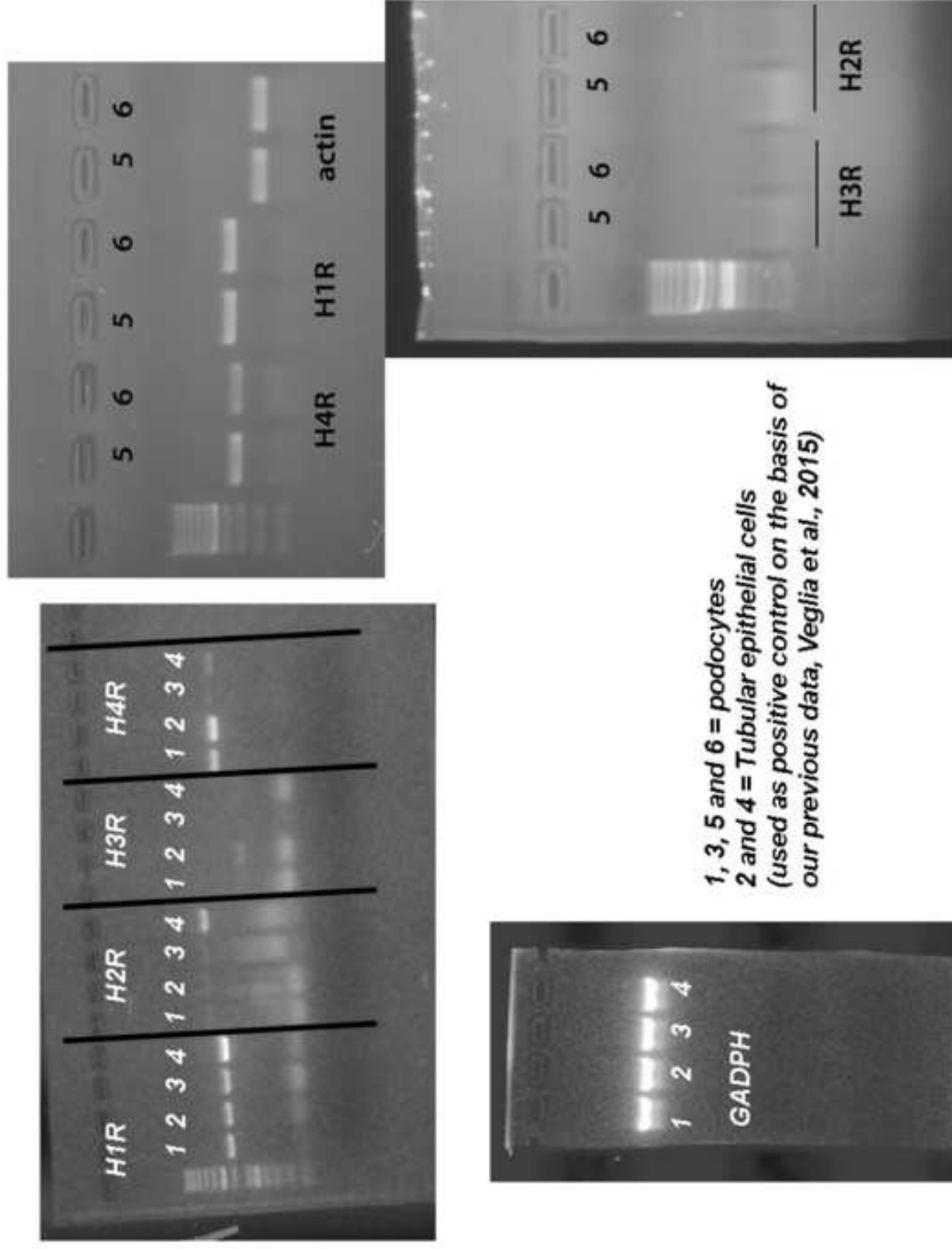


Supplementary Material Fig. 4. H₄R expression on human immortalized podocyte plasma membrane. Representative maximum projection of the Z sections from 3 independent experiments where cells were labelled with the Santa Cruz anti-H₄R antibody (Y19, sc-33967; green), and CellMask™ Plasma Membrane Stains (red). Nuclei were stained with Hoescht (blue). All the slides were examined at ×63 magnification using the SP5 Confocal Laser Scanning Microscope SMD (Leica).

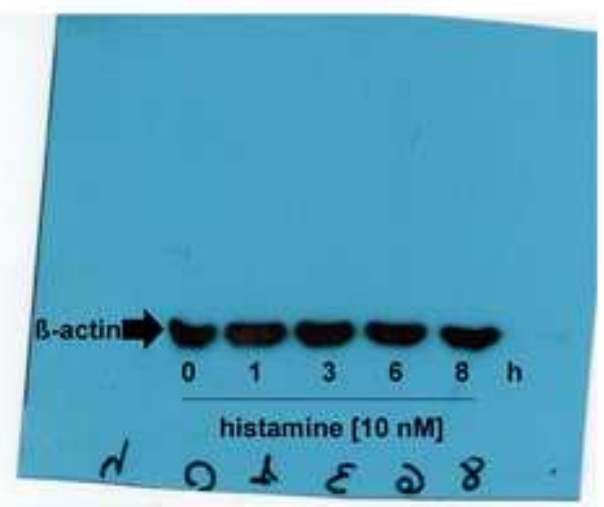
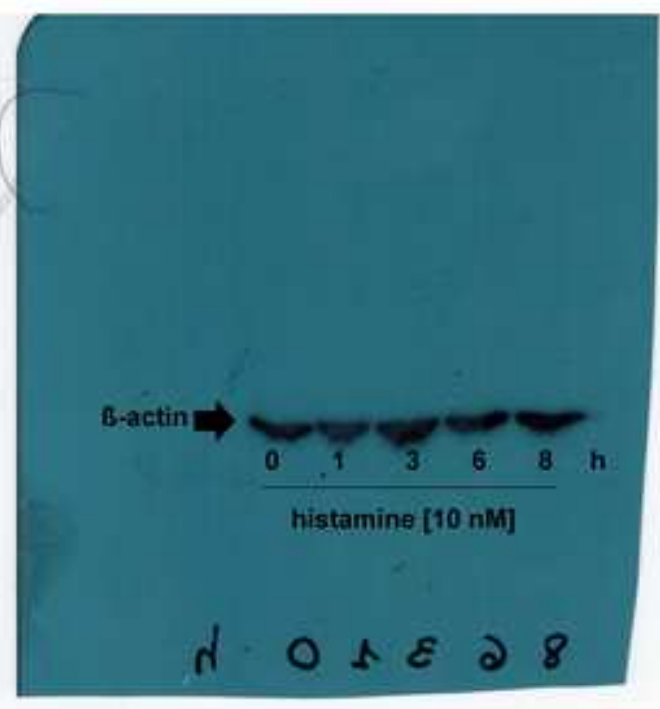
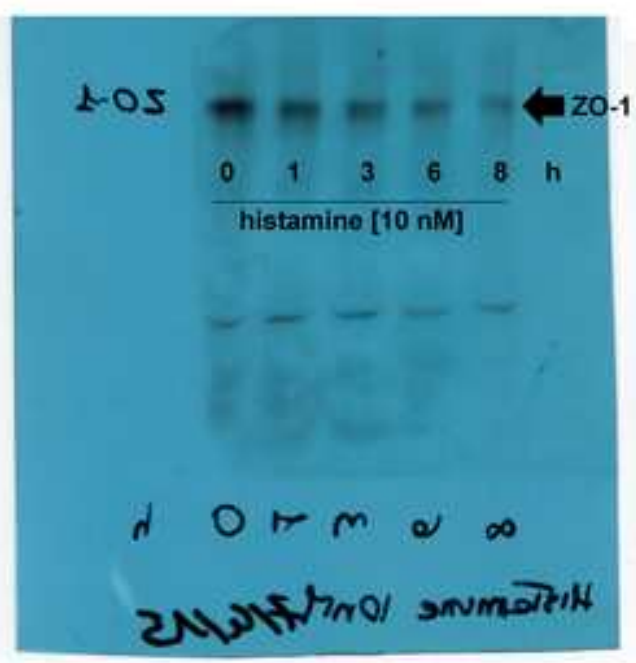


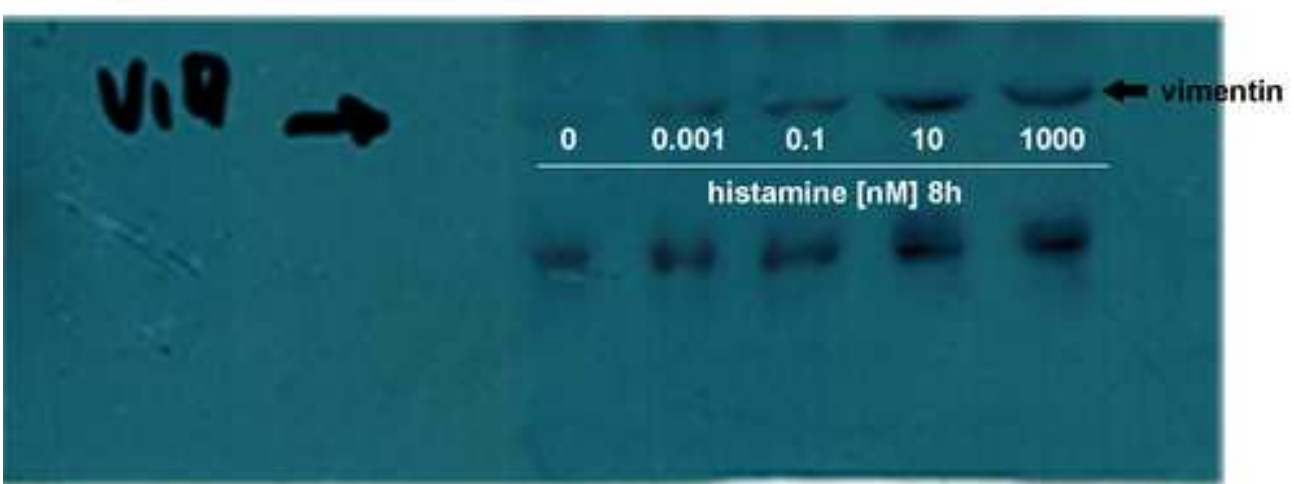
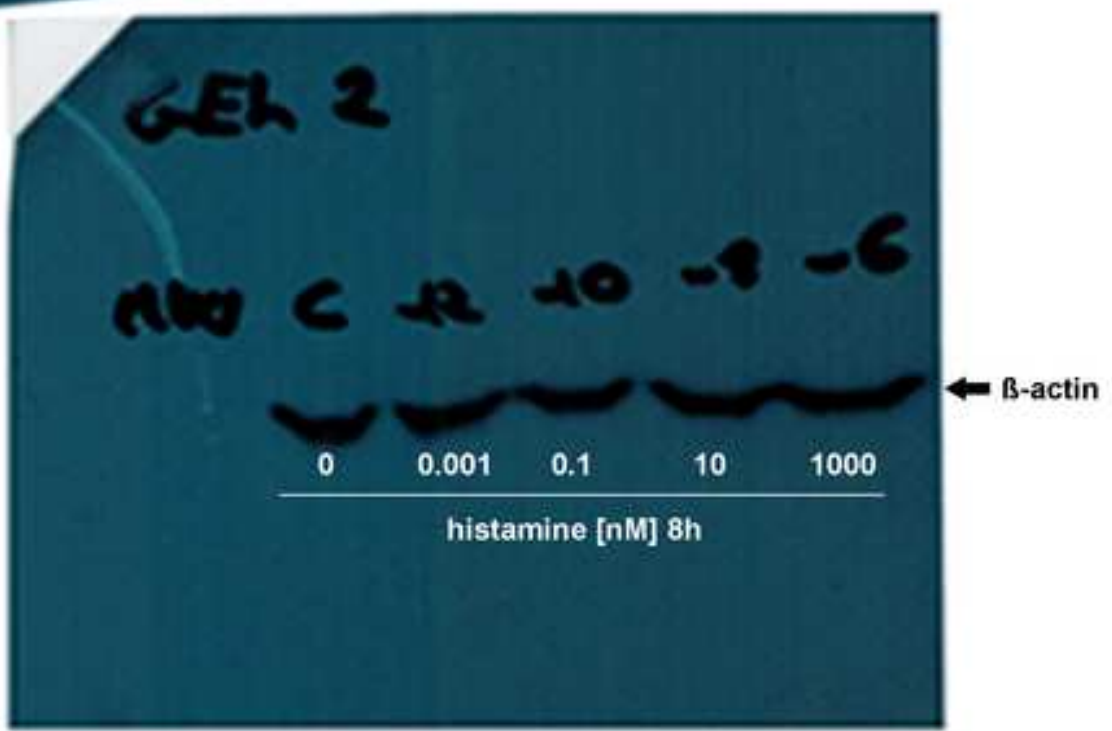
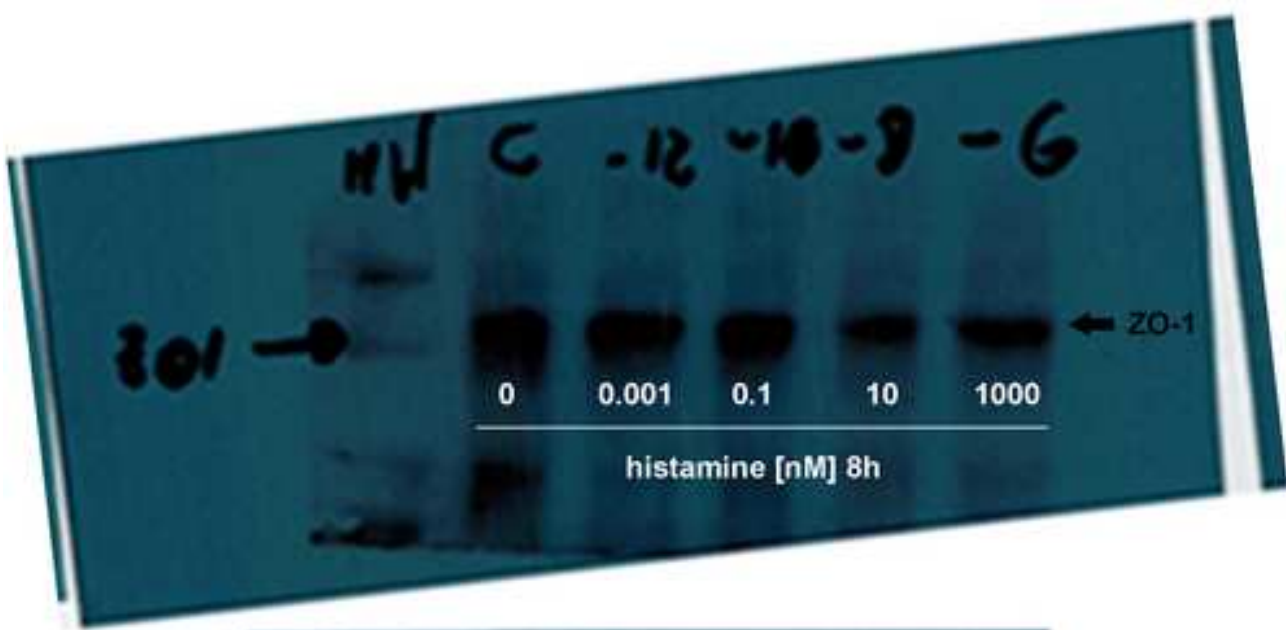
Supplementary Material Fig. 5 Ranitidine and JNJ7777120 antagonism on ZO-1, P-cadherin and vimentin expression evoked by histamine. Human immortalized podocytes pretreated for 10 min with vehicle alone (black square, straight line) or ranitidine (selective H₂R antagonist; black triangle, dotted line) or JNJ7777120 (selective H₄R antagonist; white rhombus, dashed line) 10 μ M were treated with histamine for 8 h and processed for ZO-1 (a), P-cadherin (b) and vimentin (c) protein expression. Results, represented as best-fit dose-response curve, are expressed as mean \pm SEM of 5 different experiments.





1, 3, 5 and 6 = podocytes
2 and 4 = Tubular epithelial cells
(used as positive control on the basis of
our previous data, Veglia et al., 2015)





*Supplementary Figure
[Click here to download high resolution image](#)





Conflicts of Interest Statement

Manuscript title: _____

Uncontrolled Histamine Type 1-Receptor activation of podocytes affects human Glomerular Slit Diaphragm Integrity

The authors whose names are listed immediately below certify that they have NO affiliations with or involvement in any organization or entity with any financial interest (such as honoraria; educational grants; participation in speakers' bureaus; membership, employment, consultancies, stock ownership, or other equity interest; and expert testimony or patent-licensing arrangements), or non-financial interest (such as personal or professional relationships, affiliations, knowledge or beliefs) in the subject matter or materials discussed in this manuscript.

Author names:

Eleonora Veglia, Alessandro Pini, Aldo Moggio, Cristina Grange, Federica Premoselli, Gianluca Miglio, Ekaterina Tiligada, Roberto Fantozzi, Paul L. Chazot, Arianna Carolina Rosa

The authors whose names are listed immediately below report the following details of affiliation or involvement in an organization or entity with a financial or non-financial interest in the subject matter or materials discussed in this manuscript. Please specify the nature of the conflict on a separate sheet of paper if the space below is inadequate.

Author names:

This statement is signed by all the authors to indicate agreement that the above information is true and correct (a photocopy of this form may be used if there are more than 10 authors):

Author's name (typed)	Author's signature	Date
<u>Eleonora Veglia</u>	<u>Eleonora Veglia</u>	<u>01-08-2016</u>
<u>Alessandro Pini</u>	<u>Alessandro Pini</u>	<u>01-08-2016</u>
<u>Aldo Moggio</u>	<u>Aldo Moggio</u>	<u>01-08-2016</u>
<u>Cristina Grange</u>	<u>Cristina Grange</u>	<u>01-08-2016</u>
<u>Federica Premoselli</u>	<u>Federica Premoselli</u>	<u>01-08-2016</u>
<u>Roberto Fantozzi</u>	<u>Roberto Fantozzi</u>	<u>01-08-2016</u>
<u>Paul L Chazot</u>	<u>P Chazot</u>	<u>01-08-2016</u>
<u>Arianna Carolina Rosa</u>	<u>Arianna Carolina Rosa</u>	<u>01-08-2016</u>
<u>Etiligada Katerina</u>	<u>Etiligada Katerina</u>	<u>01-08-2016</u>
<u>Gianluca Miglio</u>	<u>Gianluca Miglio</u>	<u>11-10-2016</u>